Chapter 7

Processes Resulting from the Intensity-Dependent Refractive Index

In this chapter, we explore several processes of practical importance that occur as a result of the intensity-dependent refractive index.

7.1 Self-Focusing of Light and Other Self-Action Effects

Self-focusing of light is the process in which an intense beam of light modifies the optical properties of a material medium in such a manner that the beam is caused to come to a focus within the material Kelley (1965). This circumstance is shown schematically in Fig. 7.1.1(a). Here we have assumed that n_2 is positive. As a result, the laser beam induces a refractive index variation within the material with a larger refractive index at the center of the beam than at its periphery. The material thus acts as if it were a positive lens, causing the beam to come to a focus within the material. More generally, one refers to self-action effects as effects in which a beam of light modifies its own propagation by means of the nonlinear response of a material medium. An extensive review of self-focusing is presented by Boyd et al. (2009). See especially the preface for an overview of self-action effects.

Another self-action effect is the self-trapping of light, which is illustrated in Fig. 7.1.1(b). In this process a beam of light propagates with a constant diameter as a consequence of an exact balance between self-focusing and diffraction effects. An analysis of this circumstance, which is presented below, shows that self-trapping can occur only if the power carried by the beam is exactly equal to the so-called critical power for self-trapping

$$P_{\mathrm{cr}} = \frac{\pi (0.61)^2 \lambda_0^2}{8 n_0 n_2}, \tag{7.1.1}$$

where λ_0 is the vacuum wavelength of the laser radiation. This line of reasoning leads to the conclusion that self-focusing can occur only if the beam power P is greater than P_{cr}.

Nonlinear Optics. https://doi.org/10.1016/B978-0-12-811002-7.00016-3

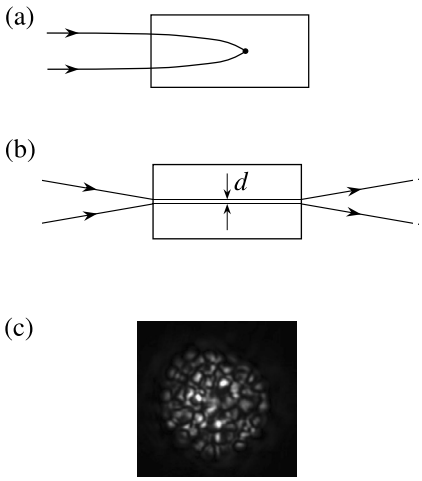

FIGURE 7.1.1: Schematic illustration of three self-action effects: (a) self-focusing of light, (b) self-trapping of light, and (c) laser beam breakup, showing the transverse distribution of intensity of a beam that has broken up into many filaments.

The final self-action effect shown in Fig. 7.1.1(c) is laser beam breakup.* This process occurs only for $P \gg P_{\rm cr}$ and leads to the breakup of the beam into many components, each of which carries a power of approximately $P_{\rm cr}$. This process occurs as a consequence of the growth of imperfections of the laser wavefront by means of the amplification associated with the forward four-wave mixing process.

Let us begin our analysis of self-action effects by developing a simple model of the self-focusing process. For the present, we ignore the effects of diffraction; these effects are introduced below. The neglect of diffraction is justified if the beam diameter or intensity (or both) is sufficiently large. Fig. 7.1.2 shows a collimated beam of light of characteristic radius w_0 and an on-axis intensity I_0 falling onto a nonlinear optical material for which n_2 is positive. We want to determine the distance $z_{\rm sf}$ from the input face of the material to the self-focus point. We make use of Fermat's principle, which in the present context states that the optical path length $\int n(\mathbf{r})\, dl$ of all rays traveling from a wavefront at the input face to the self-focus point must be equal. As a first approximation, we take the refractive index along the marginal ray to be the linear refractive index n_0 of the medium and the refractive index along the central ray

* Many authors use the term *filamentation* (or small-scale filamentation) to describe the quasi-random breakup of a laser beam into many individual components. However, other authors use the term filamentation to mean the collapse of a laser beam into a single filament, that is, the creation of a self-trapped beam of light. To avoid ambiguity, in the present work we avoid the use of the word filamentation, preferring instead to speak of laser beam breakup for the first meaning and self-trapped beams for the second.

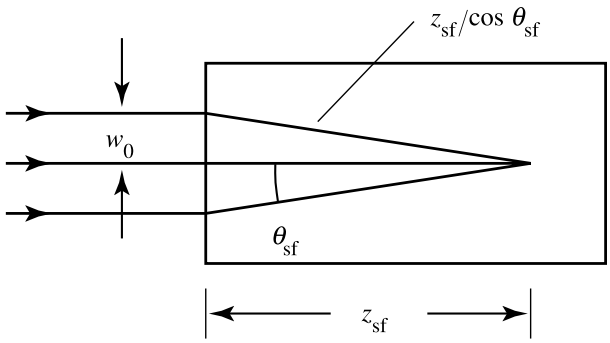

FIGURE 7.1.2: Prediction of the self-focusing distance z_{sf} by means of Fermat's principle. The curved ray trajectories within the nonlinear material are approximated as straight lines.

to be $n_0 + n_2 I_0$. Fermat's principle then tells us that

$$(n_0 + n_2 I) z_{sf} = n_0 z_{sf}/\cos\theta_{sf}, \tag{7.1.2}$$

where θ_{sf} is the angle defined in the figure. If we approximate $\cos\theta_{sf}$ as $1 - \frac{1}{2}\theta_{sf}^2$ and solve the resulting expression for θ_{sf}, we find that

$$\theta_{sf} = \sqrt{2n_2 I/n_0}. \tag{7.1.3}$$

This quantity is known as the self-focusing angle and in general can be interpreted as the characteristic angle through which a beam of light is deviated as a consequence of self-action effects. The ratio $n_2 I/n_0$ of nonlinear to linear refractive index is invariably a small quantity, thus justifying the use of the paraxial approximation. In terms of the self-focusing angle, we can calculate the characteristic self-focusing distance as $z_{sf} = w_0/\theta_{sf}$ or as

$$z_{sf} = w_0\sqrt{\frac{n_0}{2n_2 I}} = \frac{2n_0 w_0^2}{\lambda_0}\frac{1}{\sqrt{P/P_{cr}}} \quad (\text{for } P \gg P_{cr}), \tag{7.1.4}$$

where in writing the result in the second form we have made use of expression (7.1.1).

The derivation leading to the result given by Eq. (7.1.4) ignores the effects of diffraction, and thus might be expected to be valid when self-action effects overwhelm those of diffraction—that is, for $P \gg P_{cr}$. For smaller laser powers, the self-focusing distance can be estimated by noting that the beam convergence angle is reduced by diffraction effects and is given approximately by $\theta = (\theta_{sf}^2 - \theta_{dif}^2)^{1/2}$, where

$$\theta_{dif} = 0.61\lambda_0/n_0 d \tag{7.1.5}$$

is the diffraction angle of a beam of diameter d and vacuum wavelength λ_0. Then, once again arguing that $z_{sf} = w_0/\theta$, we find that

$$z_{sf} = \frac{2n_0 w_0^2}{\lambda_0} \frac{1}{\sqrt{P/P_{cr} - 1}}. \tag{7.1.6}$$

Yariv (1975) has shown that for the still more general case in which the beam has arbitrary power and arbitrary beam-waist position, the distance from the entrance face to the position of the self-focus is given by the formula

$$z_{sf} = \frac{\frac{1}{2}kw^2}{(P/P_{cr} - 1)^{1/2} + 2z_{min}/kw_0^2}, \tag{7.1.7}$$

where $k = n_0\omega/c$. The beam radius parameters w and w_0 (which have their conventional meanings) and z_{min} are defined in Fig. 7.1.3.

Even under conditions whereby a light beam does not come to a complete focus, nonlinear propagation effects can lead to a modification of the beam parameters such as the radius of curvature of the wavefront. The resulting modification of the beam shape underlies the Z-scan procedure for performing accurate measurements of the n_2 coefficient. The Z-scan method is explored in detail in Problem 3 at the end of this chapter.

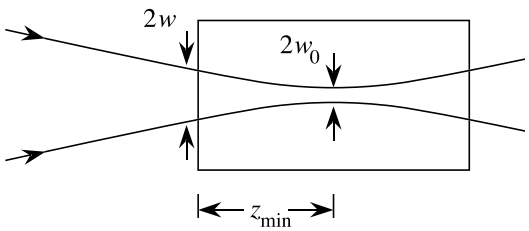

FIGURE 7.1.3: Definition of the parameters w, w_0, and z_{min}. The "rays" are shown as unmodified by the nonlinear interaction.

7.1.1 Self-Trapping of Light

Let us next consider the conditions under which self-trapping of light can occur. One expects self-trapping to occur when the tendency of a beam to spread as a consequence of diffraction is precisely balanced by the tendency of the beam to contract as a consequence of self-focusing effects. The condition for self-trapping can thus be expressed mathematically as a statement that the diffraction angle of Eq. (7.1.5) be equal to the self-focusing angle of Eq. (7.1.3)—that is, that

$$\theta_{dif} = \theta_{sf}. \tag{7.1.8}$$

By introducing Eqs. (7.1.3) and (7.1.5) into this equality, we find that self-trapping will occur only if the intensity of the light within the beam is given by

$$I = \frac{(0.61)^2 \lambda_0^2}{2 n_2 n_0 d^2}. \tag{7.1.9}$$

Since the power contained in such a beam is given by $P = (\pi/4) d^2 I$, we also see that self-trapping occurs only if the power contained in the beam has the critical value

$$P_{\mathrm{cr}} = \frac{\pi (0.61)^2 \lambda_0^2}{8 n_0 n_2} \approx \frac{\lambda_0^2}{8 n_0 n_2}. \tag{7.1.10}$$

This result was stated above without proof as Eq. (7.1.1). Note that according to the present model a self-trapped beam can have any diameter d, and that for any value of d the power contained in the filament has the same value, given by Eq. (7.1.10). The value of the numerical coefficient appearing in this formula depends on the detailed assumptions of the mathematical model of self-focusing; this issue has been discussed in detail by Fibich and Gaeta (2000).

The process of laser-beam self-trapping can be described perhaps more physically in terms of an argument presented by Chiao et al. (1964). One makes the simplifying assumption that the laser beam has a flat-top intensity distribution, as shown in Fig. 7.1.4(a). The refractive index distribution within the nonlinear medium then has the form shown in part (b) of the figure, which shows a cut through the medium that includes the symmetry axis of the laser beam. Here the refractive index of the bulk of the material is denoted by n_0 and the refractive index of that part of the medium exposed to the laser beam is denoted by $n_0 + \delta n$, where δn is the nonlinear contribution to the refractive index. Also shown in part (b) of the figure is a ray of light incident on the boundary between the two regions. It is one ray of the bundle of rays that makes up the laser beam. This ray will remain trapped within the laser beam if it undergoes total internal reflection at the boundary between the two regions. Total internal reflection occurs if θ is less than the critical angle θ_0 for total internal reflection, which is given by the equation

$$\cos \theta_0 = \frac{n_0}{n_0 + \delta n}. \tag{7.1.11}$$

Since δn is very much smaller than n_0 for essentially all nonlinear optical materials, and consequently θ_0 is much smaller than unity, Eq. (7.1.11) can be approximated by

$$1 - \tfrac{1}{2}\theta_0^2 = 1 - \frac{\delta n}{n_0},$$

which shows that the critical angle is related to the nonlinear change in refractive index by

$$\theta_0 = (2 \delta n / n_0)^{1/2}. \tag{7.1.12}$$

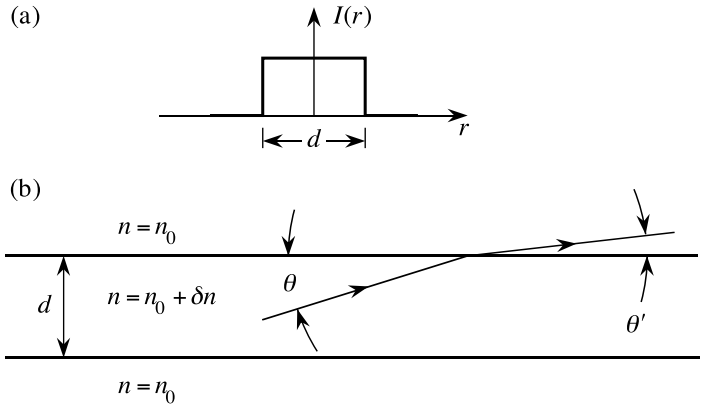

FIGURE 7.1.4: (a) Radial intensity distribution of a "flat-top" laser beam. (b) A ray of light incident on the boundary formed by the edge of the laser beam.

Note that if we identify δn with $n_2 I$, the critical angle is identical to the self-focusing angle of Eq. (7.1.3).

A laser beam of diameter d will contain rays within a cone whose maximum angular extent is of the order of the characteristic diffraction angle $\theta_{\text{dif}} = 0.61\lambda_0/n_0 d$, where λ_0 is the wavelength of the light in vacuum. We expect that self-trapping will occur if all of the rays contained in the beam undergo total internal reflection, that is, if $\theta_{\text{dif}} = \theta_0$. By comparing Eqs. (7.1.12) and (7.1.5), we see that self-trapping will occur if

$$\delta n = \tfrac{1}{2} n_0 (0.61\lambda_0/d n_0)^2, \tag{7.1.13a}$$

or equivalently, if

$$d = 0.61\lambda_0 (2n_0 \delta n)^{-1/2}. \tag{7.1.13b}$$

If we now replace δn by $n_2 I$, we see that the diameter of a self-trapped beam is related to the intensity of the light within the beam by

$$d = 0.61\lambda_0 (2n_0 n_2 I)^{-1/2}. \tag{7.1.14}$$

The power contained in a beam whose diameter is given by Eq. (7.1.14) is given as before by

$$P_{\text{cr}} = \frac{\pi}{4} d^2 I = \frac{\pi (0.61)^2 \lambda_0^2}{8 n_0 n_2}. \tag{7.1.15}$$

Note that the *power*, not the *intensity*, of the laser beam is crucial in determining whether self-focusing will occur.

When the power P greatly exceeds the critical power P_{cr} and self-focusing does occur, the beam will usually break up into many filaments, each of which contains power P_{cr}. The theory of filament formation has been described by Bespalov and Talanov (1966) and is described more fully in a following subsection.

It is instructive to determine the numerical values of the various physical quantities introduced in this section. For carbon disulfide (CS_2), n_2 for linearly polarized light is equal to 3.2×10^{-18} m^2/W, n_0 is equal to 1.7, and P_{cr} at a wavelength of 1 μm is equal to 27 kW. For typical crystals and glasses, n_2 is in the range 5×10^{-20} to 5×10^{-19} m^2/W and P_{cr} is in the range 0.2 to 2 MW. We can also estimate the self-focusing distance of Eq. (7.1.4). A fairly modest Q-switched Nd:YAG laser operating at a wavelength of 1.06 μm might produce an output pulse containing 10 mJ of energy with a pulse duration of 10 nsec, and thus with a peak power of the order of 1 MW. If we take w_0 equal to 100 μm, Eq. (7.1.4) predicts that z_{sf} is equal to 1 cm for carbon disulfide.

7.1.2 Mathematical Description of Self-Action Effects

The description of self-action effects just presented has been of a somewhat qualitative nature. Self-action effects can be described more rigorously by means of the nonlinear optical wave equation.

For the present, we consider steady-state conditions only, as would apply for excitation with a continuous-wave or long-pulse laser beam. The paraxial wave equation under these conditions is given according to Eq. (2.10.3) by

$$2ik_0 \frac{\partial A}{\partial z} + \nabla_T^2 A = -\frac{\omega^2}{\epsilon_0 c^2} p_{NL}, \tag{7.1.16}$$

where for a purely third-order nonlinear optical response the amplitude of the nonlinear polarization is given by

$$p_{NL} = 3\epsilon_0 \chi^{(3)} |A|^2 A. \tag{7.1.17}$$

Steady-state self-trapping can be described by these equations.

We consider first the solution of Eqs. (7.1.16) and (7.1.17) for a beam that is allowed to vary in one transverse dimension only. Such a situation could be realized experimentally for the situation in which a light field is constrained to propagate within a planar waveguide. In this case these equations become

$$2ik_0 \frac{\partial A}{\partial z} + \frac{\partial^2 A}{\partial x^2} = -3\chi^{(3)} \frac{\omega^2}{c^2} |A|^2 A, \tag{7.1.18}$$

where A is now a function of x and z only. This equation possesses a solution of the form

$$A(x, z) = A_0 \operatorname{sech}(x/x_0) e^{i\gamma z}, \tag{7.1.19}$$

where the width of the field distribution is given by

$$x_0 = \frac{1}{k_0}\sqrt{\frac{n_0}{2\overline{n}_2|A_0|^2}} = \frac{1}{k_0}\sqrt{\frac{n_0}{n_2 I}} \tag{7.1.20}$$

and the rate of nonlinear phase acquisition is given by

$$\gamma = k_0 \overline{n}_2 |A_0|^2 / n_0 = k_0 n_2 I/(2n_0), \tag{7.1.21}$$

where, as in Section 4.1, $\overline{n}_2 = 3\chi^{(3)}/4n_0$ and $n_2 I = 2\overline{n}_2|A_0|^2$. The solution given by Eq. (7.1.19) is sometimes referred to as a spatial soliton, because it describes a field that can propagate for long distances with an invariant transverse profile. Behavior of this sort has been observed experimentally by Barthelemy et al. (1985) and by Aitchison et al. (1991).

For a beam that varies in both transverse directions, Eqs. (7.1.16) and (7.1.17) cannot be solved analytically, and only numerical results are known. The lowest-order solution for a beam with cylindrical symmetry was reported by Chiao et al. (1964) and is of the form of a bell-shaped curve of approximately gaussian shape. Detailed analysis shows that in two transverse dimensions spatial solitons are unstable in a pure Kerr medium (i.e., one described by an $\overline{n}_2$ nonlinearity) but that they can propagate stably in a saturable nonlinear medium. Stable self-trapping in saturable media has been observed experimentally by Bjorkholm and Ashkin (1974). Higher-order solutions have been reported by Haus (1966).

7.1.3 Laser Beam Breakup into Many Filaments

We mentioned earlier that beam breakup occurs as a consequence of the growth by forward four-wave-mixing amplification of irregularities initially present on the laser wavefront. This occurrence is illustrated schematically in Fig. 7.1.5. Beam breakup typically leads to the generation of a beam with a random intensity distribution, of the sort shown in part (c) of Fig. 7.1.1.

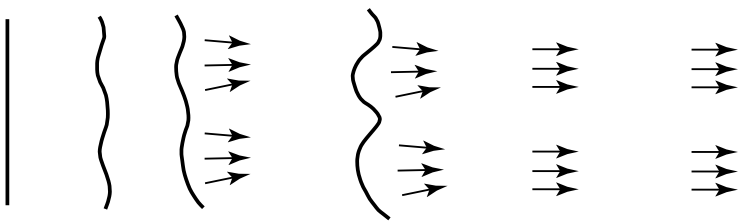

FIGURE 7.1.5: Illustration of laser beam breakup by the growth of wavefront perturbations.

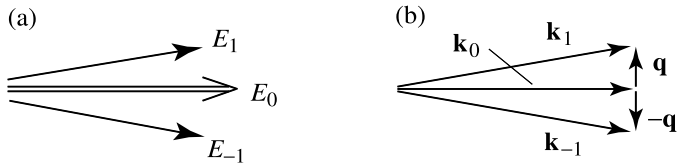

FIGURE 7.1.6: (a) Beam breakup occurs by the growth of the spatial sidemodes E_1 and E_{-1} at the expense of the strong central component E_0. (b) Wavevectors of the interacting waves.

However, under certain circumstances, the beam breakup process can produce beams with a transverse structure in the form of highly regular geometrical patterns; see, for instance, Bennink et al. (2002).

Let us now present a mathematical description of the process of laser beam breakup. Our derivation follows closely that of the original description of Bespalov and Talanov (1966). We begin by expressing the field within the nonlinear medium as

$$\tilde{E}(\mathbf{r}, t) = E(\mathbf{r})e^{-i\omega t} + \text{c.c.}, \tag{7.1.22}$$

where (see also Fig. 7.1.6) it is convenient to express the electric field amplitude as the sum of three plane-wave components as

$$\begin{aligned} E(\mathbf{r}) &= E_0(\mathbf{r}) + E_1(\mathbf{r}) + E_{-1}(\mathbf{r}) = \left[A_0(z) + A_1(\mathbf{r}) + A_{-1}(\mathbf{r})\right]e^{ikz} \\ &= \left[A_0(z) + a_1(z)e^{i\mathbf{q}\cdot\mathbf{r}} + a_{-1}(z)e^{-i\mathbf{q}\cdot\mathbf{r}}\right]e^{ikz}, \end{aligned} \tag{7.1.23}$$

where $k = n_0\omega/c$. Here E_0 represents the strong central component of the laser field and E_1 and E_{-1} represent weak, symmetrically displaced spatial sidemodes; at various points in the calculation it will prove useful to make use of the related quantities A_0, $A_{\pm 1}$ and $a_{\pm 1}$ which are introduced in the last form of this expression. The latter quantities are defined in relation to the transverse component $\mathbf{q}$ of the optical wavevector of the off-axis modes. We next calculate the nonlinear polarization in the usual manner:

$$P = 3\epsilon_0\chi^{(3)}|E|^2E \equiv P_0 + P_1 + P_{-1}, \tag{7.1.24}$$

where the part of the polarization that is phase matched to the strong central component is given by

$$P_0 = 3\epsilon_0\chi^{(3)}|E_0|^2E_0 = 3\epsilon_0\chi^{(3)}|A_0|^2A_0\,e^{ikz} \equiv p_0e^{ikz}, \tag{7.1.25}$$

and where the part of the polarization that is phase matched to the sidemodes is given by

$$P_{\pm 1} = 3\epsilon_0\chi^{(3)}\left(2|E_0|^2E_{\pm 1} + E_0^2E_{\mp 1}^*\right) \equiv p_{\pm 1}e^{ikz}. \tag{7.1.26}$$

We first solve the wave equation for the spatial evolution of A_0, which is described by

$$2ik\frac{\partial A_0}{\partial z} + \nabla_\perp^2 A_0 = -\frac{\omega^2}{\epsilon_0 c^2} p_0. \tag{7.1.27}$$

We have assumed that A_0 is a uniform plane wave, and thus $\nabla_\perp^2 A_0 = 0$. The solution of the resulting equation is

$$A_0(z) = A_{00} e^{i\gamma z}, \tag{7.1.28}$$

where

$$\gamma = \frac{3\omega\chi^{(3)}}{2n_0 c}|A_{00}|^2 = n_2 k_{\text{vac}} I \tag{7.1.29}$$

denotes the spatial rate of nonlinear phase acquisition and where we have made use of the form of n_2 given by Eq. (4.1.19). This solution expresses the expected result that the strong central component simply acquires a nonlinear phase shift as it propagates. We now use this result with Eq. (7.1.26) to find that the part of the nonlinear polarization that couples to the sidemodes is given by

$$p_{\pm 1} = 3\epsilon_0 \chi^{(3)}\left[2|A_{00}|^2 A_{\pm 1} + A_{00}^2 e^{2i\gamma z} A_{\mp 1}^*\right]. \tag{7.1.30}$$

We next consider the wave equation for the off-axis modes. Starting with

$$2ik\frac{\partial A_{\pm 1}}{\partial z} + \nabla_\perp^2 A_{\pm 1} = -\frac{\omega^2}{\epsilon_0 c^2} p_{\pm 1}, \tag{7.1.31}$$

we introduce $A_{\pm 1} = a_{\pm 1}\exp(\pm i\mathbf{q}\cdot\mathbf{r})$ and expression (7.1.30) for $P_{\pm 1}$ to obtain

$$2ik\frac{\partial a_{\pm 1}}{\partial z} - q^2 a_{\pm 1} = -\frac{\omega^2}{c^2} 3\chi^{(3)}|A_{00}|^2\left[2a_{\pm 1} + a_{\mp 1}^* e^{2i\gamma z}\right]. \tag{7.1.32}$$

This equation is now rearranged, and expression (7.1.29) for γ is introduced to obtain

$$\frac{da_{\pm 1}}{dz} + \frac{iq^2}{2k} a_{\pm 1} = i\gamma\left(2a_{\pm 1} + a_{\mp 1}^* e^{2i\gamma z}\right). \tag{7.1.33}$$

We next perform a change of variables to remove the unwanted exponential phase factor appearing in the last term in this equation. In particular, we define

$$a_{\pm 1} = a'_{\pm 1} e^{i\gamma z}. \tag{7.1.34}$$

In terms of the new "primed" variables, Eq. (7.1.33) becomes

$$\frac{d}{dz} a'_{\pm 1} = i\left(\gamma - q^2/2k\right) a'_{\pm 1} + i\gamma a'^*_{\mp 1}. \tag{7.1.35}$$

This set of equations now possesses constant coefficients and can be solved directly. Perhaps the simplest way to solve these equations is to express them in matrix form as

$$\frac{d}{dz}\begin{bmatrix} a_1' \\ a_{-1}'^* \end{bmatrix} = \begin{bmatrix} i(\gamma-\beta) & i\gamma \\ -i\gamma & -i(\gamma-\beta) \end{bmatrix}\begin{bmatrix} a_1' \\ a_{-1}'^* \end{bmatrix}, \tag{7.1.36}$$

where $\beta \equiv q^2/2k$. We seek the eigensolutions of this equation—that is, solutions of the form

$$\begin{bmatrix} a_1'(z) \\ a_{-1}'^*(z) \end{bmatrix} = \begin{bmatrix} a_1'(0) \\ a_{-1}'^*(0) \end{bmatrix} e^{\Lambda z}. \tag{7.1.37}$$

The parameter Λ is the gain eigenvalue. The real part of Λ gives the spatial growth rate (if positive) or the attenuation rate (if negative) of the coupled solution. This assumed solution is substituted into Eq. (7.1.36), which then becomes

$$\begin{bmatrix} i(\gamma-\beta)-\Lambda & i\gamma \\ -i\gamma & -i(\gamma-\beta)-\Lambda \end{bmatrix}\begin{bmatrix} a_1'(0) \\ a_{-1}'^*(0) \end{bmatrix} = 0. \tag{7.1.38}$$

This equation possesses nonvanishing solutions only if the determinant of the two-by-two matrix appearing in this equation vanishes. This condition leads to the result that

$$\Lambda = \pm\sqrt{\beta(2\gamma-\beta)}. \tag{7.1.39}$$

Note that this system of equations can produce gain ($\mathrm{Re}\,\Lambda > 0$) only for $\gamma > \frac{1}{2}\beta$, which shows immediately that n_2 must be positive in order for beam breakup to occur. More explicitly, Fig. 7.1.7 shows a plot of the forward four-wave-mixing gain coefficient Λ as a function of the transverse wavevector magnitude q. We see that the maximum gain is numerically equal to the nonlinear phase shift γ experienced by the pump wave. We also see that the gain vanishes for all values of q greater than $q_{\max} = 2\sqrt{k\gamma}$ and reaches its maximum value for wavevector $q_{\mathrm{opt}} = q_{\max}/\sqrt{2}$. There is consequently a characteristic angle at which the breakup process occurs, which is given by

$$\theta_{\mathrm{opt}} = q_{\mathrm{opt}}/k. \tag{7.1.40}$$

This angle has a direct physical interpretation, as described originally by Chiao et al. (1966). In particular, θ_{opt} is the direction in which the near-forward four-wave-mixing process becomes phase matched, when account is taken of the nonlinear contributions to the wavevectors of the on- and off-axis waves.

It is instructive to calculate the characteristic power carried by each of the filaments created by the breakup process. This power P_{fil} is of the order of the initial intensity I of the laser beam times the characteristic cross sectional area of one of the filaments. We identify this area

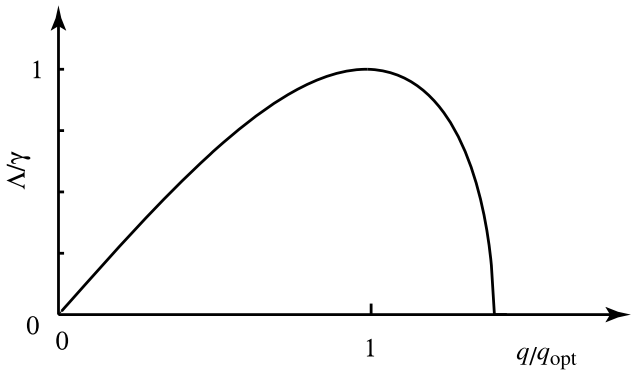

FIGURE 7.1.7: Variation of the gain coefficient Λ of the forward four-wave mixing process that leads to laser-beam breakup with the transverse wavevector magnitude q.

with the square of the characteristic transverse distance scale associated with the beam breakup process—that is, with $w_{\text{eff}}^2 = (\pi/q)^2$. We thereby find that

$$P_{\text{fil}} = \frac{\lambda^2}{8n_0 n_2}, \tag{7.1.41}$$

which is very nearly equal to the critical power for self-focusing P_{cr} introduced in Eq. (7.1.1). We thus see that the beam breakup process is one in which the laser beam breaks up into a large number of individual components, each of which carries power of the order of P_{cr}.

Conditions for the Occurrence of Nonlinear Beam Breakup

Let us next determine the conditions under which laser beam breakup is expected to occur. This issue is quite subtle for the following reasons. First, the breakup process grows from perturbations initially present on the laser wavefront, and thus a very clean laser beam will have a much higher threshold for beam breakup than a "dirty" beam. Second, whereas the gain of the breakup process depends directly on laser intensity, the properties of whole-beam self-focusing depend on the intensity and beam spot size in a more complicated manner.

To address this question, we define a beam breakup distance z_{br} by means of the relation $n_2 k_{\text{vac}} I z_{\text{br}} = G$, where G is a numerical factor (of the order of 3 to 10) that specifies the level of gain that must be present in order for beam breakup to occur. For the optimum transverse wavevector q_{opt}, the gain coefficient Λ attains its maximum value $\Lambda = \gamma = n_2 k_{\text{vac}} I$, and we thus find that

$$z_{\text{br}} = \frac{G}{n_2 k_{\text{vac}} I}. \tag{7.1.42}$$

This distance is to be compared to the self-focusing distance

$$z_{\mathrm{sf}} = \frac{2n_0 w_0^2}{\lambda_0} \frac{1}{\sqrt{P/P_{\mathrm{cr}} - 1}} \tag{7.1.43}$$

(see Eq. (7.1.4) derived earlier), with $P_{\mathrm{cr}} = \pi(0.61)^2\lambda_0^2/8n_0n_2$. The condition for the occurrence of beam breakup then can be stated as $z_{\mathrm{fil}} < L$, where L is the interaction path length, and $z_{\mathrm{fil}} < z_{\mathrm{sf}}$. These conditions state that the breakup process must occur within the length of the interaction region, and that the competing process of whole-beam self-focusing must *not* occur. Note that z_{fil} decreases more rapidly with increasing laser power (or intensity) than does z_{sf}, and thus beam breakup can always be induced through use of a sufficiently large laser power. We now calculate the value of the laser power under conditions such that z_{br} is exactly equal to z_{sf}. We find, using Eq. (7.1.43) in the limit $P \gg P_{\mathrm{cr}}$, that

$$P/P_{\mathrm{cr}} = 4G^2. \tag{7.1.44}$$

For the representative value $G = 5$, we find that beam breakup is expected only for $P > 100P_{\mathrm{cr}}$.

7.1.4 Self-Action Effects with Pulsed Laser Beams

For simplicity and conceptual clarity, the preceding discussion has dealt with continuous-wave laser beams. Self-action effects can have quite a different character when excited using pulsed radiation. Only some general comments are presented here. Additional aspects of self-action effects as excited by ultrashort optical pulses are presented in Chapter 13.

Moving Focus Model

The moving focus model was developed by Loy and Shen (1973) to describe the properties of self-focusing when excited with nanosecond laser pulses. To understand this model, one notes that for pulsed radiation the self-focusing distance z_{sf} of Eq. (7.1.4) (i.e., the distance from the input face of the nonlinear medium to the self-focus point) will vary according to the value of the instantaneous intensity $I(t)$ at the input face. Thus, the focal point will sweep through the material as it follows the temporal evolution of the pulse intensity. Under many circumstances, damage will occur at the point of peak intensity, and thus the damage tracks observed by early works (Hercher, 1964) can be interpreted as the locus of focal points for all values of the input intensity $I(t)$. Some aspects of the moving focus model are quite subtle. For instance, because of transit time effects, there are typically two self-focal points within the material at any given moment of time. One of these occurs closer to the entrance face of the material and is a consequence of intense light near the peak of the pulse, whereas another focus occurs at greater distances into the material and occurs as a consequence of earlier, weaker parts of the pulse.

Transient Self-Focusing

Transient self-focusing occurs when the laser pulse duration τ_p is comparable to or shorter than the turn-on time of the material response. In this situation, the nonlinear response develops during the temporal extent of the laser pulse, and consequently the nonlinear response is stronger for the trailing edge of the pulse than for the leading edge. Thus the trailing edge is more strongly self-focused than is the leading edge, leading to significant distortion of the pulse intensity distribution in both space and time. This process has been described in detail by Shen (1975). Transient self-focusing can be observed, for example, through use of picosecond laser pulses propagating through liquids in which the dominant nonlinearity is the molecular orientation effect.

7.2 Optical Phase Conjugation

Optical phase conjugation is a process that can be used to remove the effects of aberrations from certain types of optical systems (Zel'dovich et al., 1985; Boyd and Grynberg, 1992). The nature of the phase conjugation process is illustrated in Fig. 7.2.1. Part (a) of the figure shows an optical wave falling at normal incidence onto an ordinary metallic mirror. We see that the most advanced portion of the incident wavefront remains the most advanced in the reflected wave. Part (b) of the figure shows the same wavefront falling onto a phase-conjugate mirror. In this case the most advanced portion turns into the most retarded portion in the reflection process. For this reason, optical phase conjugation is sometimes referred to as wavefront reversal. Note, however, that the wavefront is reversed only with respect to normal geometrical reflection; in fact, the generated wavefront exactly replicates the incident wavefront but propagates in the opposite direction. For this reason, optical phase conjugation is also sometimes referred to as the generation of a time-reversed wavefront, as shown more explicitly in Eq. (7.2.5).

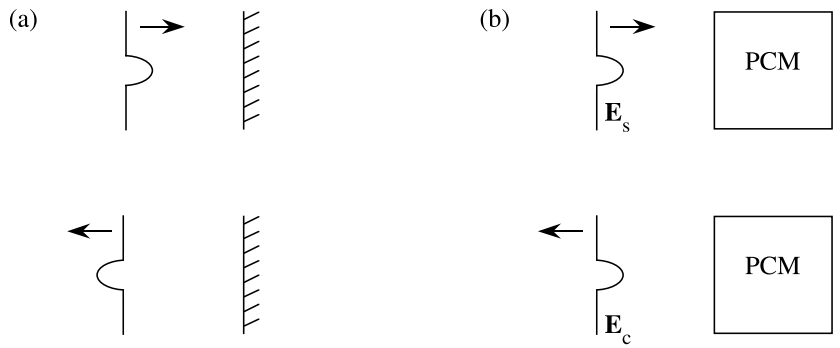

FIGURE 7.2.1: Reflection from (a) an ordinary mirror and (b) a phase-conjugate mirror.

The reason why the process illustrated in part (b) of Fig. 7.2.1 is called phase conjugation can be understood by introducing a mathematical description of the process. We represent the wave incident on the phase-conjugate mirror (called the signal wave) as

$$\tilde{\mathbf{E}}_{\mathrm{s}}(\mathbf{r}, t) = \mathbf{E}_{\mathrm{s}}(\mathbf{r}) e^{-i\omega t} + \text{c.c.} \tag{7.2.1}$$

When illuminated by such a wave, a phase-conjugate mirror produces a reflected wave, called the phase-conjugate wave, described by

$$\tilde{\mathbf{E}}_{\mathrm{c}}(\mathbf{r}, t) = r\mathbf{E}_{\mathrm{s}}^{*}(\mathbf{r}) e^{-i\omega t} + \text{c.c.}, \tag{7.2.2}$$

where r represents the amplitude reflection coefficient of the phase-conjugate mirror. In order to determine the significance of replacing $\mathbf{E}_{\mathrm{s}}(\mathbf{r})$ by $\mathbf{E}_{\mathrm{s}}^{*}(\mathbf{r})$ in the reflection process, it is useful to represent $\mathbf{E}_{\mathrm{s}}(\mathbf{r})$ as the product

$$\mathbf{E}_{\mathrm{s}}(\mathbf{r}) = \hat{\boldsymbol{\epsilon}}_{\mathrm{s}} A_{\mathrm{s}}(\mathbf{r}) e^{i\mathbf{k}_{\mathrm{s}} \cdot \mathbf{r}}, \tag{7.2.3}$$

where $\hat{\boldsymbol{\epsilon}}_{\mathrm{s}}$ represents the polarization unit vector, $A_{\mathrm{s}}(\mathbf{r})$ the slowly varying field amplitude, and $\mathbf{k}_{\mathrm{s}}$ the mean wavevector of the incident light. The complex conjugate of Eq. (7.2.3) is given explicitly by

$$\mathbf{E}_{\mathrm{s}}^{*}(\mathbf{r}) = \hat{\boldsymbol{\epsilon}}_{\mathrm{s}}^{*} A_{\mathrm{s}}^{*}(\mathbf{r}) e^{-i\mathbf{k}_{\mathrm{s}} \cdot \mathbf{r}}. \tag{7.2.4}$$

We thus see that the action of an ideal phase-conjugate mirror is threefold:

1. The complex polarization unit vector of the incident radiation is replaced by its complex conjugate. For example, right-hand circular light remains right-hand circular in reflection from a phase-conjugate mirror rather than being converted into left-hand circular light, as is the case in reflection at normal incidence from a metallic mirror.
2. $A_{\mathrm{s}}(\mathbf{r})$ is replaced by $A_{\mathrm{s}}^{*}(\mathbf{r})$, implying that the wavefront is reversed in the sense illustrated in Fig. 7.2.1(b).*
3. $\mathbf{k}_{\mathrm{s}}$ is replaced by $-\mathbf{k}_{\mathrm{s}}$, showing that the incident wave is reflected back into its direction of incidence. From the point of view of ray optics, this result shows that each ray of the incident beam is precisely reflected back onto itself.

Note further that Eqs. (7.2.1) through (7.2.4) imply that

$$\tilde{\mathbf{E}}_{\mathrm{c}}(\mathbf{r}, t) = r\tilde{\mathbf{E}}_{\mathrm{s}}(\mathbf{r}, -t). \tag{7.2.5}$$

This result shows that the phase conjugation process can be thought of as the generation of a time-reversed wavefront.

* Because of this property, the phase conjugation process displays special quantum noise characteristics. These characteristics have been described by Gaeta and Boyd (1988).

It is important to note that the description given by Eq. (7.2.4) refers to an *ideal* phase-conjugate mirror. Many physical devices that are commonly referred to as phase-conjugate mirrors are imperfect either in the sense that they do not possess all three of these properties or in the sense that they possess these properties only approximately. For example, many phase-conjugate mirrors are highly imperfect in their polarization properties, even though they are nearly perfect in their ability to perform wavefront reversal.

7.2.1 Aberration Correction by Phase Conjugation

The process of phase conjugation is able to remove the effects of aberrations under conditions such that a beam of light passes twice in opposite directions through an aberrating medium. The reason why optical phase conjugation leads to aberration correction is illustrated in Fig. 7.2.2. Here an initially plane wavefront propagates through an aberrating medium. The aberration may be due to turbulence in the earth's atmosphere, inhomogeneities in the refractive index of a piece of glass, or a poorly designed optical system. The wavefront of the light leaving the medium therefore becomes distorted in the manner shown schematically in the figure. If this aberrated wavefront is now allowed to fall onto a phase-conjugate mirror, a conjugate wavefront will be generated, and the sense of the wavefront distortion will be inverted in this reflected wave. As a result, when this wavefront passes through the aberrating medium again, an undistorted output wave will emerge.

Let us now see how to demonstrate mathematically that optical phase conjugation leads to aberration correction. (Our treatment here is similar to that of Yariv and Fisher in Fisher, 1983.) We consider a wave $\tilde{E}(\mathbf{r}, t)$ propagating through a lossless material of nonuniform refractive index $n(\mathbf{r}) = [\epsilon(\mathbf{r})]^{1/2}$, as shown in Fig. 7.2.3.

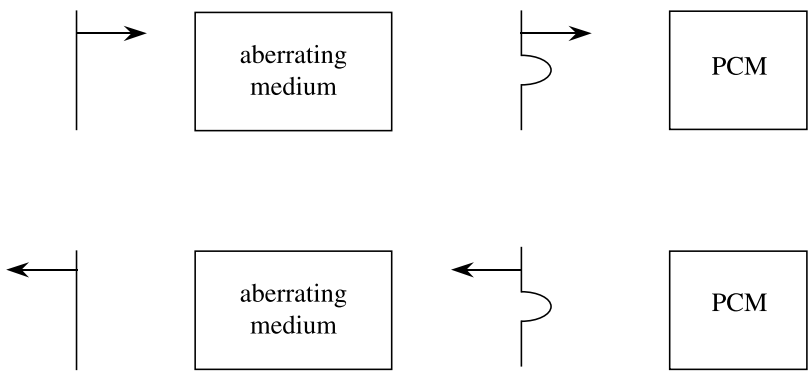

FIGURE 7.2.2: Aberration correction by optical phase conjugation.

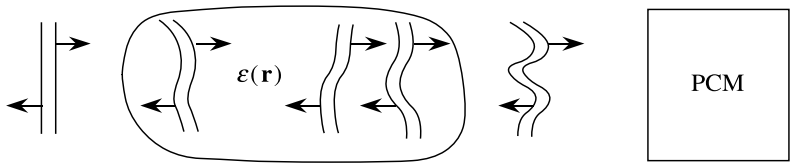

FIGURE 7.2.3: Conjugate waves propagating through an inhomogeneous optical medium.

We assume that the spatial variation of $\epsilon(\mathbf{r})$ occurs on a scale that is much larger than an optical wavelength. The optical field in this region must obey the wave equation, which we write in the form

$$\nabla^2 \tilde{E} - \frac{\epsilon(\mathbf{r})}{c^2}\frac{\partial^2 \tilde{E}}{\partial t^2} = 0. \tag{7.2.6}$$

We represent the field propagating to the right through this region as

$$\tilde{E}(\mathbf{r}, t) = A(\mathbf{r})e^{i(kz-\omega t)} + \text{c.c.}, \tag{7.2.7}$$

where the field amplitude $A(\mathbf{r})$ is assumed to be a slowly varying function of $\mathbf{r}$. Since we have singled out the z direction as the mean direction of propagation, it is convenient to express the Laplacian operator that appears in Eq. (7.2.6) as

$$\nabla^2 = \frac{\partial^2}{\partial z^2} + \nabla_T^2, \tag{7.2.8}$$

where $\nabla_T^2 = \partial^2/\partial x^2 + \partial^2/\partial y^2$ is called the transverse Laplacian. Eqs. (7.2.7) and (7.2.8) are now introduced into Eq. (7.2.6), which becomes

$$\nabla_T^2 A + \left[\frac{\omega^2 \epsilon(\mathbf{r})}{c^2} - k^2\right]A + 2ik\frac{\partial A}{\partial z} = 0. \tag{7.2.9}$$

In writing this equation in the form shown, we have omitted the term $\partial^2 A/\partial z^2$ because $A(\mathbf{r})$ has been assumed to be slowly varying. Since this equation is generally valid, so is its complex conjugate, which is given explicitly by

$$\nabla_T^2 A^* + \left[\frac{\omega^2 \epsilon(\mathbf{r})}{c^2} - k^2\right]A^* - 2ik\frac{\partial A^*}{\partial z} = 0. \tag{7.2.10}$$

However, this equation describes the wave

$$\tilde{E}_c(\mathbf{r}, t) = A^*(\mathbf{r})e^{i(-kz-\omega t)} + \text{c.c.}, \tag{7.2.11}$$

which is a wave propagating in the negative z direction whose complex amplitude is *everywhere* the complex conjugate of the forward-going wave. This proof shows that if the phase-conjugate

mirror can generate a backward-going wave whose amplitude is the complex conjugate of that of the forward-going wave at any one plane (say the input face of the mirror), then the field amplitude of the backward-going wave will be the complex conjugate of that of the forward-going wave at *all* points in front of the mirror. In particular, if the forward-going wave is a plane wave before entering the aberrating medium, then the backward-going (i.e., conjugate) wave emerging from the aberrating medium will also be a plane wave.

The phase conjugation process is directly suited for removing the effects of aberrations in double pass, but under special circumstances can be used to perform single-pass aberration correction; see, for instance, MacDonald et al. (1988).

7.2.2 Phase Conjugation by Degenerate Four-Wave Mixing

Let us now consider a physical process that can produce a phase conjugate wavefront. It has been shown by Hellwarth (1977) and by Yariv and Pepper (1977) that the phase conjugate of an incident wave can be created by the process of degenerate four-wave mixing (DFWM) using the geometry shown in Fig. 7.2.4. This four-wave mixing process is degenerate in the sense that all four interacting waves have the same frequency. In this process, a lossless nonlinear medium characterized by a third-order nonlinear susceptibility $\chi^{(3)}$ is illuminated by two strong counterpropagating pump waves E_1 and E_2 and by a signal wave E_3. The pump waves are usually taken to be plane waves, although in principle they can possess any wavefront structure as long as their amplitudes are complex conjugates of one another. The signal wave is allowed to have an arbitrary wavefront. In this section we show that, as a result of the nonlinear coupling between these waves, a new wave E_4 is created that is the phase conjugate of E_3. We also derive an expression (Eq. (7.2.37)) that describes the efficiency with which the conjugate wave is generated.

Since the following mathematical development is somewhat involved, it is useful to first consider in simple terms why the interaction illustrated in Fig. 7.2.4 leads to the generation of

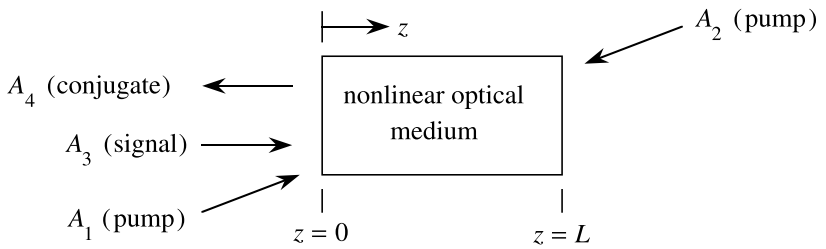

FIGURE 7.2.4: Geometry of phase conjugation by degenerate four-wave mixing.

a conjugate wavefront. We represent the four interacting waves by

$$\begin{aligned}\tilde{E}_i(\mathbf{r},t) &= E_i(\mathbf{r})e^{-i\omega t} + \text{c.c.} \\ &= A_i(\mathbf{r})e^{i(\mathbf{k}_i\cdot\mathbf{r}-\omega t)} + \text{c.c.}\end{aligned} \tag{7.2.12}$$

for $i = 1, 2, 3, 4$, where the $A_i(\mathbf{r})$ are slowly varying quantities. The nonlinear polarization produced within the medium by the three input waves will have, in addition to a large number of other terms, a term of the form

$$P^{\text{NL}} = 6\epsilon_0\chi^{(3)}E_1E_2E_3^* = 6\epsilon_0\chi^{(3)}A_1A_2A_3^*e^{i(\mathbf{k}_1+\mathbf{k}_2-\mathbf{k}_3)\cdot\mathbf{r}}. \tag{7.2.13}$$

We have assumed that the pump waves E_1 and E_2 are counterpropagating, and thus their wavevectors are related by

$$\mathbf{k}_1 + \mathbf{k}_2 = 0, \tag{7.2.14}$$

and thus Eq. (7.2.13) becomes

$$P^{\text{NL}} = 6\epsilon_0\chi^{(3)}A_1A_2A_3^*e^{-i\mathbf{k}_3\cdot\mathbf{r}}. \tag{7.2.15}$$

We see that this contribution to the nonlinear polarization has a spatial dependence that allows it to act as a phase-matched source term for a conjugate wave (E_4) having wavevector $-\mathbf{k}_3$, and we thus see that the wavevectors of the signal and conjugate waves are related by

$$\mathbf{k}_3 = -\mathbf{k}_4. \tag{7.2.16}$$

The field amplitude of the wave generated by the nonlinear polarization of Eq. (7.2.15) will be proportional to $A_1A_2A_3^*$. This wave will be the phase conjugate of A_3 whenever the phase of the product A_1A_2 is spatially invariant, either because A_1 and A_2 both represent plane waves and hence are each constant or because A_1 and A_2 are phase conjugates of one another (because if A_2 is proportional to A_1^*, then A_1A_2 will be proportional to the real quantity $|A_1|^2$).

We can also understand the interaction shown in Fig. 7.2.4 from the following point of view. The incoming signal wave of amplitude A_3 interferes with one of the pump waves (e.g., the forward-going pump wave of amplitude A_1) to form a spatially varying intensity distribution. As a consequence of the nonlinear response of the medium, a refractive index variation accompanies this interference pattern. This variation acts as a volume diffraction grating, which scatters the other pump wave to form the outgoing conjugate wave of amplitude A_4.

Let us now treat the degenerate four-wave mixing process more rigorously. The total field amplitude within the nonlinear medium is given by

$$E = E_1 + E_2 + E_3 + E_4. \tag{7.2.17}$$

This field produces a nonlinear polarization within the medium, given by

$$P = 3\epsilon_0 \chi^{(3)} E^2 E^*, \tag{7.2.18}$$

where $\chi^{(3)} = \chi^{(3)}(\omega = \omega + \omega - \omega)$. The product $E^2 E^*$ that appears on the right-hand side of this equation contains a large number of terms with different spatial dependences. Those terms with spatial dependence of the form

$$e^{i\mathbf{k}_i \cdot \mathbf{r}} \quad \text{for } i = 1, 2, 3, 4 \tag{7.2.19}$$

are particularly important because they can act as phase-matched source terms for one of the four interacting waves. The polarization amplitudes associated with these phase-matched contributions are as follows:

$$\begin{aligned}
P_1 &= 3\epsilon_0 \chi^{(3)} \left[E_1^2 E_1^* + 2E_1 E_2 E_2^* + 2E_1 E_3 E_3^* + 2E_1 E_4 E_4^* + 2E_3 E_4 E_2^* \right], \\
P_2 &= 3\epsilon_0 \chi^{(3)} \left[E_2^2 E_2^* + 2E_2 E_1 E_1^* + 2E_2 E_3 E_3^* + 2E_2 E_4 E_4^* + 2E_3 E_4 E_1^* \right], \\
P_3 &= 3\epsilon_0 \chi^{(3)} \left[E_3^2 E_3^* + 2E_3 E_1 E_1^* + 2E_3 E_2 E_2^* + 2E_3 E_4 E_4^* + 2E_1 E_2 E_4^* \right], \\
P_4 &= 3\epsilon_0 \chi^{(3)} \left[E_4^2 E_4^* + 2E_4 E_1 E_1^* + 2E_4 E_2 E_2^* + 2E_4 E_3 E_3^* + 2E_1 E_2 E_3^* \right].
\end{aligned} \tag{7.2.20}$$

We next assume that the fields E_3 and E_4 are much weaker than the pump fields E_1 and E_2. In the above expressions we therefore drop those terms that contain more than one weak-field amplitude. We hence obtain

$$\begin{aligned}
P_1 &= 3\epsilon_0 \chi^{(3)} \left[E_1^2 E_1^* + 2E_1 E_2 E_2^* \right], \\
P_2 &= 3\epsilon_0 \chi^{(3)} \left[E_2^2 E_2^* + 2E_2 E_1 E_1^* \right], \\
P_3 &= 3\epsilon_0 \chi^{(3)} \left[2E_3 E_1 E_1^* + 2E_3 E_2 E_2^* + 2E_1 E_2 E_4^* \right], \\
P_4 &= 3\epsilon_0 \chi^{(3)} \left[2E_4 E_1 E_1^* + 2E_4 E_2 E_2^* + 2E_1 E_2 E_3^* \right].
\end{aligned} \tag{7.2.21}$$

Note that, at the present level of approximation, the E_3 and E_4 fields are each driven by a polarization that depends on the amplitudes of all of the fields, but that the polarizations driving the E_1 and E_2 fields depend only on E_1 and E_2 themselves. We thus consider first the problem of calculating the spatial evolution of the pump field amplitudes E_1 and E_2. We can then later use these known amplitudes when we calculate the spatial evolution of the signal and conjugate waves.

We assume that each of the interacting waves obeys the wave equation in the form

$$\nabla^2 \tilde{E}_i - \frac{\epsilon}{c^2} \frac{\partial^2 \tilde{E}_i}{\partial t^2} = \frac{1}{\epsilon_0 c^2} \frac{\partial^2}{\partial t^2} \tilde{P}_i. \tag{7.2.22}$$

We now introduce Eqs. (7.2.12) and (7.2.21) into this equation and make the slowly varying amplitude approximation. Also, we let z' be the spatial coordinate measured in the direction

of propagation of the E_1 field, and we assume for simplicity that the pump waves have plane wavefronts. We then find that the pump field A_1 must obey the equation

$$\left[\left(-k_1^2 + 2ik_1\frac{d}{dz'} + \frac{\epsilon\omega^2}{c^2}\right)A_1\right]e^{i(k_1z'-\omega t)} = -\frac{\omega^2}{c^2}\,3\chi^{(3)}\left[|A_1|^2 + 2|A_2|^2\right]A_1e^{i(k_1z'-\omega t)},$$

which, after simplification, becomes

$$\frac{dA_1}{dz'} = \frac{3i\omega}{2nc}\chi^{(3)}\left[|A_1|^2 + 2|A_2|^2\right]A_1 \equiv i\kappa_1A_1. \tag{7.2.23a}$$

We similarly find that the backward-going pump wave is described by the equation

$$\frac{dA_2}{dz'} = \frac{-3i\omega}{2nc}\chi^{(3)}\left[|A_2|^2 + 2|A_1|^2\right]A_2 \equiv i\kappa_2A_2. \tag{7.2.23b}$$

Since κ_1 and κ_2 are real quantities, these equations show that A_1 and A_2 each undergo phase shifts as they propagate through the nonlinear medium. The phase shift experienced by each wave depends both on its own intensity and on that of the other wave. Note that each wave shifts the phase of the other wave by twice as much as it shifts its own phase, in consistency with the general result described in the discussion following Eq. (4.1.14). These phase shifts can induce a phase mismatch into the process that generates the phase-conjugate signal. Note that since only the phases (and not the amplitudes) of the pump waves are affected by the nonlinear coupling, the quantities $|A_1|^2$ and $|A_2|^2$ are spatially invariant, and thus the quantities κ_1 and κ_2 that appear in Eqs. (7.2.23) are in fact constants. These equations can therefore be solved directly to obtain

$$A_1(z') = A_1(0)e^{i\kappa_1z'}, \tag{7.2.24a}$$

$$A_2(z') = A_2(0)e^{-i\kappa_2z'}. \tag{7.2.24b}$$

The product A_1A_2 that appears in the expression (7.2.15) for the nonlinear polarization responsible for producing the phase-conjugate wave therefore varies spatially as

$$A_1(z')A_2(z') = A_1(0)A_2(0)e^{i(\kappa_1-\kappa_2)z'}; \tag{7.2.25}$$

the factor $e^{i(\kappa_1-\kappa_2)z'}$ shows the effect of wavevector mismatch. If the two pump beams have equal intensities so that $\kappa_1 = \kappa_2$, the product A_1A_2 becomes spatially invariant, so that

$$A_1(z')A_2(z') = A_1(0)A_2(0), \tag{7.2.26}$$

and in this case the interaction is perfectly phase-matched. We shall henceforth assume that the pump intensities are equal.

We next consider the coupled-amplitude equations describing the signal and conjugate fields, $\tilde{E}_3$ and $\tilde{E}_4$. We assume for simplicity that the incident signal wave has plane wavefronts. This is actually not a restrictive assumption, because an arbitrary signal field can be decomposed into plane-wave components, each of which will couple to a plane-wave component of the conjugate field $\tilde{E}_4$. Under this assumption, the wave equation (7.2.22) applied to the signal and conjugate fields leads to the coupled-amplitude equations

$$\frac{dA_3}{dz} = \frac{3i\omega}{nc}\chi^{(3)}\left[\left(|A_1|^2 + |A_2|^2\right)A_3 + A_1A_2A_4^*\right], \tag{7.2.27a}$$

$$\frac{dA_4}{dz} = -\frac{3i\omega}{nc}\chi^{(3)}\left[\left(|A_1|^2 + |A_2|^2\right)A_4 + A_1A_2A_3^*\right]. \tag{7.2.27b}$$

For convenience, we write these equations as

$$\frac{dA_3}{dz} = i\kappa_3 A_3 + i\kappa A_4^*, \tag{7.2.28a}$$

$$\frac{dA_4}{dz} = -i\kappa_3 A_4 - i\kappa A_3^*, \tag{7.2.28b}$$

where we have introduced the coupling coefficients

$$\kappa_3 = \frac{3\omega}{nc}\chi^{(3)}\left(|A_1|^2 + |A_2|^2\right), \tag{7.2.29a}$$

$$\kappa = \frac{3\omega}{nc}\chi^{(3)}A_1A_2. \tag{7.2.29b}$$

The set of equations (7.2.28) can be simplified through a change of variables. We let

$$A_3 = A_3'e^{i\kappa_3 z}, \tag{7.2.30a}$$

$$A_4 = A_4'e^{-i\kappa_3 z}. \tag{7.2.30b}$$

Note that the primed and unprimed variables coincide at the input face of the interaction region—that is, at the plane $z = 0$. We introduce these relations into Eq. (7.2.28a) which becomes

$$i\kappa_3 A_3'e^{i\kappa_3 z} + \frac{dA_3'}{dz}e^{i\kappa_3 z} = i\kappa_3 A_3'e^{i\kappa_3 z} + i\kappa A_4'^*e^{i\kappa_3 z},$$

or

$$\frac{dA_3'}{dz} = i\kappa A_4'^*. \tag{7.2.31a}$$

We similarly find that Eq. (7.2.28b) becomes

$$\frac{dA_4'}{dz} = -i\kappa A_3'^*. \tag{7.2.31b}$$

This set of equations shows why degenerate four-wave mixing leads to phase conjugation: The generated field A_4' is driven only by the complex conjugate of the input field amplitude. We note that this set of equations is *formally* identical to the set that we would have obtained if we had taken the driving polarizations of Eq. (7.2.21) to be simply

$$P_1 = P_2 = 0, \qquad P_3 = 6\epsilon_0 \chi^{(3)} E_1 E_2 E_4^*, \qquad P_4 = 6\epsilon_0 \chi^{(3)} E_1 E_2 E_3^*, \tag{7.2.32}$$

that is, if we had ignored the modification of the pump waves resulting from the nonlinear interaction.

Next, we solve the set of equations (7.2.31). We take the derivative of Eq. (7.2.31b) with respect to z and introduce Eq. (7.2.31a) to obtain

$$\frac{d^2 A_4'}{dz^2} + |\kappa|^2 A_4' = 0. \tag{7.2.33}$$

This result shows that the spatial dependence of A_4' must be of the form

$$A_4'(z) = B \sin|\kappa| z + C \cos|\kappa| z. \tag{7.2.34}$$

In order to determine the constants B and C, we must specify the initial condition for each of the two weak waves at its input plane. In particular, we assume that $A_3'^*(0)$ and $A_4'(L)$ are specified. In this case, the solution of Eq. (7.2.33) is

$$A_3'^*(z) = -\frac{i|\kappa|}{\kappa} \frac{\sin|\kappa| z}{\cos|\kappa| L} A_4'(L) + \frac{\cos[|\kappa|(z-L)]}{\cos|\kappa| L} A_3'^*(0), \tag{7.2.35a}$$

$$A_4'(z) = \frac{\cos|\kappa| z}{\cos|\kappa| L} A_4'(L) - \frac{i\kappa}{|\kappa|} \frac{\sin[|\kappa|(z-L)]}{\cos|\kappa| L} A_3'^*(0). \tag{7.2.35b}$$

However, for the case of four-wave mixing for optical phase conjugation, we can usually assume that there is no conjugate wave injected into the medium at $z = L$—that is, we can assume that

$$A_4'(L) = 0. \tag{7.2.36}$$

Furthermore, we are usually interested only in the output values of the two interacting fields. These output field amplitudes are then given by

$$A_3'^*(L) = \frac{A_3'^*(0)}{\cos|\kappa| L}, \tag{7.2.37a}$$

$$A_4'(0) = \frac{i\kappa}{|\kappa|} (\tan|\kappa| L) A_3'^*(0). \tag{7.2.37b}$$

Note that the transmitted signal wave $A_3'^*(L)$ is always more intense than the incident wave. Note also that the output conjugate wave $A_4(0)$ can have any intensity ranging from zero to

infinity, the actual value depending on the particular value of $|\kappa|L$. The reflectivity of a phase-conjugate mirror based on degenerate four-wave mixing can exceed 100% because the mirror is actively pumped by externally applied waves, which can supply energy.

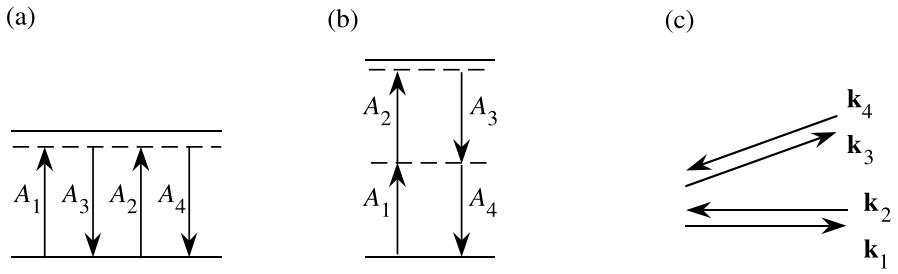

FIGURE 7.2.5: Parts (a) and (b) are energy-level diagrams describing two different interactions that can lead to phase conjugation by degenerate four-wave mixing. In either case, the interaction involves the simultaneous annihilation of two pump photons with the creation of signal and conjugate photons. Diagram (a) describes the dominant interaction if the applied field frequency is nearly resonant with a one-photon transition of the material system, whereas (b) describes the dominant interaction under conditions of two-photon-resonant excitation. Part (c) shows the wavevectors of the four interacting waves. Because $\mathbf{k}_1 + \mathbf{k}_2 - \mathbf{k}_3 - \mathbf{k}_4 = 0$, the process is perfectly phase-matched.

From the point of view of energetics, we can describe the process of degenerate four-wave mixing as a process in which one photon from each of the pump waves is annihilated and one photon is added to each of the signal and conjugate waves, as shown in Fig. 7.2.5. Hence, the conjugate wave A_4 is created, and the signal wave A_3 is amplified. The degenerate four-wave mixing process with counterpropagating pump waves is automatically phase-matched (when the two pump waves have equal intensity or whenever we can ignore the nonlinear phase shifts experienced by each wave). We see that this is true because no phase-mismatch terms of the sort $e^{\pm i\,\Delta\kappa z}$ appear on the right-hand sides of Eqs. (7.2.31). The fact that degenerate four-wave mixing in the phase conjugation geometry is automatically phase-matched has a very simple physical interpretation. Since this process entails the annihilation of two pump photons and the creation of a signal and conjugate photon, the total input energy is $2\hbar\omega$ and the total input momentum is $\hbar(\mathbf{k}_1 + \mathbf{k}_2) = 0$; consequently the total output energy must be $2\hbar\omega$ and the total output momentum must be $\hbar(\mathbf{k}_3 + \mathbf{k}_4) = 0$. If the two pump beams are not exactly counterpropagating, then $\hbar(\mathbf{k}_1 + \mathbf{k}_2)$ does not vanish and the phase-matching condition is not automatically satisfied.

The first experimental demonstration of phase conjugation by degenerate four-wave mixing was performed by Bloom and Bjorklund (1977). Their experimental setup is shown in Fig. 7.2.6. They observed that the presence of the aberrating glass plate did not lower the resolution of the system when the mirror was aligned to retroreflect the pump laser beam onto itself.

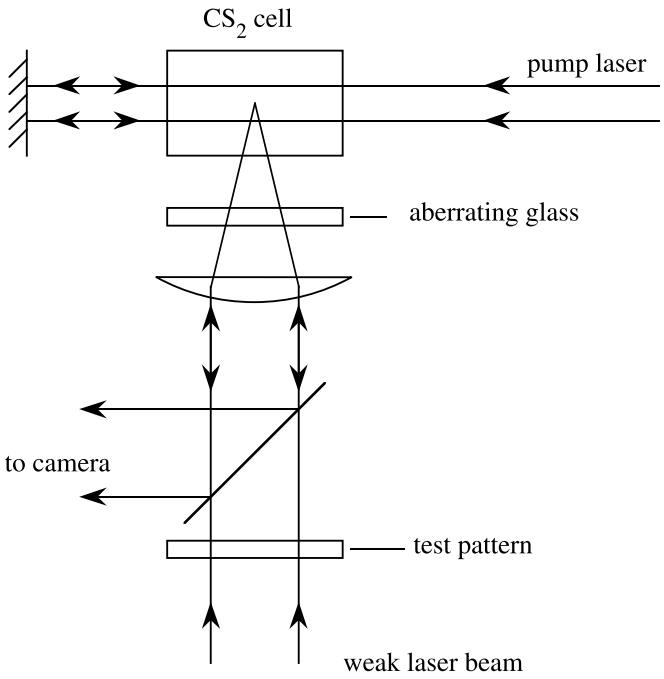

FIGURE 7.2.6: Experimental setup for studying phase conjugation by degenerate four-wave mixing.

However, when this mirror was partially misaligned, the return beam passed through a different portion of the aberrating glass and the resolution of the system was degraded.

Degenerate four-wave mixing is usually performed using the geometry of Fig. 7.2.4, although it can also be performed using the surface nonlinearity of the interface between a linear and nonlinear medium; see, for instance, Maki et al. (1992) for details.

7.2.3 Polarization Properties of Phase Conjugation

Our discussion thus far has treated phase conjugation in the scalar approximation and has shown that phase conjugation can be used to remove the effects of wavefront aberrations. It is often desirable that phase conjugation be able to remove the effects of polarization distortions as well. An example is shown in Fig. 7.2.7. Here a beam of light that initially is linearly polarized passes through a stressed optical component. As a result of stress-induced birefringence, the state of polarization of the beam becomes distorted nonuniformly over the cross section of the beam. This beam then falls onto a phase-conjugate mirror. If this mirror is ideal in the sense that the polarization unit vector $\hat{\boldsymbol{\epsilon}}$ of the incident light is replaced by its complex conjugate in the reflected beam, the effects of the polarization distortion will be removed in the second pass

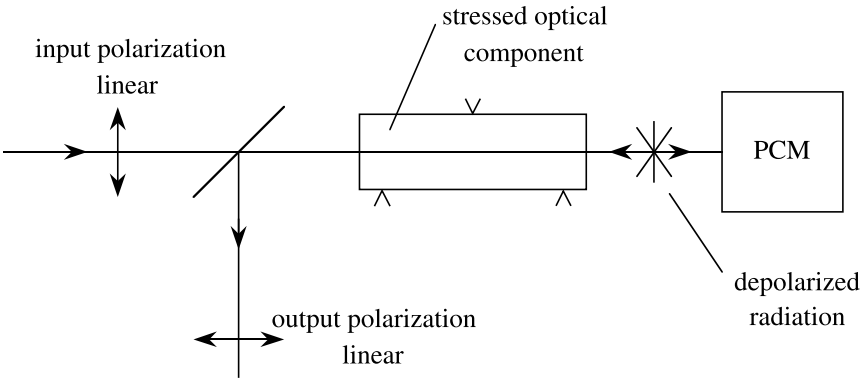

FIGURE 7.2.7: Polarization properties of phase conjugation.

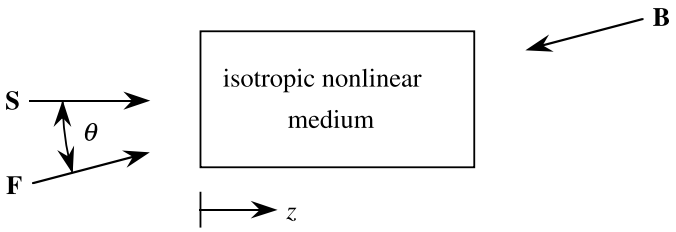

FIGURE 7.2.8: Geometry of vector phase conjugation.

through the stressed optical component, and the beam will be returned to its initial state of linear polarization. A phase-conjugate mirror that produces a reflected beam that is both a wavefront conjugate and a polarization conjugate is often called a vector phase-conjugate mirror.

In order to describe the polarization properties of the degenerate four-wave mixing process, we consider the geometry shown in Fig. 7.2.8, where **F**, **B**, and **S** denote the amplitudes of the forward- and backward-going pump waves and of the signal wave, respectively. The total applied field is thus given by

$$\mathbf{E} = \mathbf{F} + \mathbf{B} + \mathbf{S}. \tag{7.2.38}$$

We assume that the angle θ between the signal and forward-going pump wave is much smaller than unity, so that only the x and y components of the incident fields have appreciable amplitudes. We also assume that the nonlinear optical material is isotropic, so that the third-order nonlinear optical susceptibility $\chi^{(3)}_{ijkl} = \chi^{(3)}_{ijkl}(\omega = \omega + \omega - \omega)$ is given by Eq. (4.2.5) as

$$\chi^{(3)}_{ijkl} = \chi_{1122}(\delta_{ij}\delta_{kl} + \delta_{ik}\delta_{jl}) + \chi_{1221}\delta_{il}\delta_{jk}, \tag{7.2.39}$$

and so that the nonlinear polarization can be expressed as

$$\begin{aligned}\mathbf{P} &= 6\epsilon_0\chi_{1122}(\mathbf{E}\cdot\mathbf{E}^*)\mathbf{E} + 3\epsilon_0\chi_{1221}(\mathbf{E}\cdot\mathbf{E})\mathbf{E}^* \\ &= \epsilon_0 A(\mathbf{E}\cdot\mathbf{E}^*)\mathbf{E} + \tfrac{1}{2}\epsilon_0 B(\mathbf{E}\cdot\mathbf{E})\mathbf{E}^*. \end{aligned} \tag{7.2.40}$$

If we now introduce Eq. (7.2.38) into Eq. (7.2.40), we find that the phase-matched contribution to the nonlinear polarization that acts as a source for the conjugate wave is given by

$$\begin{bmatrix} P_x \\ P_y \end{bmatrix} = 6\epsilon_0 \begin{bmatrix} \chi_{1111}B_xF_x + \chi_{1221}B_yF_y & \chi_{1122}(B_xF_y + B_yF_x) \\ \chi_{1122}(B_yF_x + B_xF_y) & \chi_{1111}B_yF_y + \chi_{1221}B_xF_x \end{bmatrix} \begin{bmatrix} S_x^* \\ S_y^* \end{bmatrix}, \tag{7.2.41}$$

where $\chi_{1111} = 2\chi_{1122} + \chi_{1221}$. The polarization properties of the phase-conjugation process will be ideal (i.e., vector phase conjugation will be obtained) whenever the two-by-two transfer matrix of Eq. (7.2.41) is a multiple of the identity matrix. Under these conditions, both cartesian components of the incident field are reflected with equal efficiency, their relative phases are preserved, and no coupling takes place between orthogonal components.

There are two different ways in which the matrix in Eq. (7.2.41) can be made to reduce to a multiple of the identity matrix. One way is for $A = 6\chi_{1122}$ to vanish identically. In this case Eq. (7.2.41) becomes

$$\begin{aligned}\begin{bmatrix} P_x \\ P_y \end{bmatrix} &= 6\epsilon_0\chi_{1221}(B_xF_x + B_yF_y)\begin{bmatrix} 1 & 0 \\ 0 & 1 \end{bmatrix}\begin{bmatrix} S_x^* \\ S_y^* \end{bmatrix} \\ &= 6\epsilon_0\chi_{1221}(B_xF_x + B_yF_y)\begin{bmatrix} S_x^* \\ S_y^* \end{bmatrix}, \end{aligned} \tag{7.2.42}$$

and thus the nonlinear polarization is proportional to the complex conjugate of the signal amplitude for *any* choice of the polarization vectors of the pump waves. This result can be understood directly in terms of Eq. (7.2.40), which shows that $\mathbf{P}$ has the vector character of $\mathbf{E}^*$ whenever χ_{1122} vanishes. However, χ_{1122} (or A) vanishes identically only under very unusual circumstances. The only known case for this condition to occur is that of degenerate four-wave mixing in an atomic system utilizing a two-photon resonance between certain atomic states. This situation has been analyzed by Grynberg (1984) and Kauranen et al. (1989) and studied experimentally by Malcuit et al. (1988). The analysis can be described most simply for the case of a transition between two S states of an atom with zero electron spin. The four-wave mixing process can then be described graphically by the diagram shown in Fig. 7.2.9. Since the lower and upper levels each possess zero angular momentum, the sum of the angular momenta of the signal and conjugate photons must be zero, and this condition implies that the polarization unit vectors of the two waves must be related by complex conjugation.

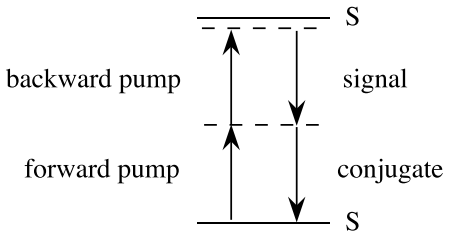

FIGURE 7.2.9: Phase conjugation by degenerate four-wave mixing using a two-photon transition.

For most physical mechanisms giving rise to optical nonlinearities, the coefficient A does not vanish. (Recall that for molecular orientation $B/A = 6$, for electrostriction $B/A = 0$, and for nonresonant electronic response $B/A = 1$.) For the general case in which A is not equal to 0, vector phase conjugation in the geometry in Fig. 7.2.8 can be obtained only when the pump waves are circularly polarized and counterrotating. By counterrotating, we mean that if the forward-going wave is described by

$$\tilde{\mathbf{F}}(z,t) = F\frac{\hat{x} - i\hat{y}}{\sqrt{2}}e^{i(kz-\omega t)} + \text{c.c.}, \tag{7.2.43a}$$

then the backward-going wave is described by

$$\tilde{\mathbf{B}}(z,t) = B\frac{\hat{x} + i\hat{y}}{\sqrt{2}}e^{i(-kz-\omega t)} + \text{c.c.} \tag{7.2.43b}$$

These waves are counterrotating in the sense that, for any fixed value of z, $\tilde{\mathbf{F}}$ rotates clockwise in time in the xy plane and $\tilde{\mathbf{B}}$ rotates counterclockwise in time. However, both waves are right-hand circularly polarized, since, by convention, the handedness of a wave is the sense of rotation as determined when looking into the beam.

In the notation of Eq. (7.2.41), the amplitudes of the fields described by (7.2.43) are given by

$$\begin{aligned} F_x &= \frac{F}{\sqrt{2}}e^{ikz}, & F_y &= -i\frac{F}{\sqrt{2}}^{ikz}, \\ B_x &= \frac{B}{\sqrt{2}}e^{-ikz}, & B_y &= i\frac{B}{\sqrt{2}}e^{-ikz}, \end{aligned} \tag{7.2.44}$$

and so Eq. (7.2.41) becomes

$$\begin{bmatrix} P_x \\ P_y \end{bmatrix} = 3\epsilon_0 FB(\chi_{1111} + \chi_{1221}) \begin{bmatrix} 1 & 0 \\ 0 & 1 \end{bmatrix} \begin{bmatrix} S_x^* \\ S_y^* \end{bmatrix}. \tag{7.2.45}$$

We see that the transfer matrix is again a multiple of the identity matrix and hence that the nonlinear polarization vector is proportional to the complex conjugate of the signal field vector. The fact that degenerate four-wave mixing excited by counterrotating pump waves leads to vector phase conjugation was predicted theoretically by Zel'dovich and Shkunov (1979) and was verified experimentally by Martin et al. (1980).

The reason why degenerate four-wave mixing with counterrotating pump waves leads to vector phase conjugation can be understood in terms of the conservation of linear and angular momentum. As just described, phase conjugation can be visualized as a process in which one photon from each pump wave is annihilated and a signal and conjugate photon are simultaneously created. Since the pump waves are counterpropagating and counterrotating, the total linear and angular momenta of the two input photons must vanish. Then conservation of linear and angular momentum requires that the conjugate wave must be emitted in a direction opposite to the direction of propagation of the signal wave and that its polarization vector must rotate in a sense opposite to that of the signal wave.

7.3 Optical Bistability and Optical Switching

Certain nonlinear optical systems can possess more than one output state for a given input state. The term *optical bistability* refers to the situation in which two different output intensities are possible for a given input intensity, and the more general term *optical multistability* is used to describe the circumstance in which two or more stable output states are possible. Interest in optical bistability stems from its potential usefulness as a memory element or a switch for use in optical communication and in optical computing.

Optical bistability was first described theoretically and observed experimentally using an absorptive nonlinearity by Szöke et al. (1969). Optical bistability was observed experimentally for the case of a refractive nonlinearity (real $\chi^{(3)}$) by Gibbs et al. (1976). The bistable optical device described in these works consists of a nonlinear medium placed inside of a Fabry–Perot resonator. Such a device is illustrated schematically in Fig. 7.3.1. Here A_1 denotes the field amplitude of the incident wave, A_1' denotes that of the reflected wave, A_2 and A_2' denote the amplitudes of the forward- and backward-going waves within the interferometer, and A_3 denotes the amplitude of the transmitted wave. The cavity mirrors are assumed to be identical and lossless, with amplitude reflectance ρ and transmittance τ that are related to the intensity reflectance R and transmittance T through

$$R = |\rho|^2 \quad \text{and} \quad T = |\tau|^2 \tag{7.3.1a}$$

with

$$R + T = 1. \tag{7.3.1b}$$

The incident and internal fields are related to each other through boundary conditions of the form

$$A_2' = \rho A_2 e^{2ikl-\alpha l}, \tag{7.3.2a}$$

$$A_2 = \tau A_1 + \rho A_2'. \tag{7.3.2b}$$

In these equations, we assume that the field amplitudes are measured at the inner surface of the left-hand mirror. The propagation constant $k = n\omega/c$ and intensity absorption coefficient α are taken to be real quantities, which include both their linear and nonlinear contributions. In writing Eq. (7.3.2) in the form shown, we have implicitly made a mean-field approximation—that is, we have assumed that the quantities k and α are spatially invariant; if such is not the case, the exponent should be replaced by $\int_0^l dz[2ik(z) - \alpha(z)]$. For simplicity we also assume that the nonlinear material and the medium surrounding the resonator have the same linear refractive indices.

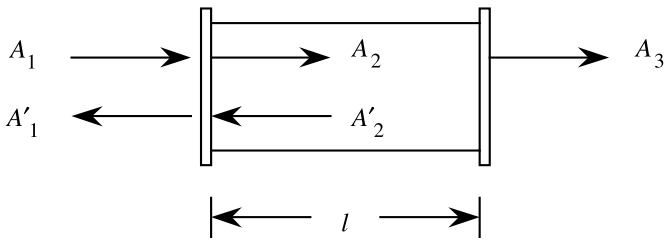

FIGURE 7.3.1: Bistable optical device in the form of a Fabry–Perot interferometer containing a nonlinear medium.

Eqs. (7.3.2) can be solved algebraically by eliminating A_2' to obtain

$$A_2 = \frac{\tau A_1}{1 - \rho^2 e^{2ikl-\alpha l}}, \tag{7.3.3}$$

which is known as Airy's function* and which describes the properties of a Fabry–Perot interferometer. If k or α (or both) is a sufficiently nonlinear function of the intensity of the light within the interferometer, this equation predicts bistability in the intensity of the transmitted wave. In general, both k and α can display nonlinear behavior; however, we can obtain a better understanding of the nature of optical bistability by considering in turn the limiting cases in which either the absorptive or the refractive contribution dominates.

* The original paper of Fabry and Perot (Ann. Chim. Phys. 12, 459, 1897) refers to this form as Airy's function but does not give a citation to the specific publication of G.B. Airy.

7.3.1 Absorptive Bistability

Let us first examine the case in which only the absorption coefficient α depends nonlinearly on the field intensity. The wavevector magnitude k is hence assumed to be constant. To simplify the following analysis, we assume that the mirror separation l is adjusted so that the cavity is tuned to resonance with the applied field; in such a case the factor $\rho^2 e^{2ikl}$ that appears in the denominator of Eq. (7.3.3) is equal to the real quantity R. We also assume that $\alpha l \ll 1$, so that we can ignore the spatial variation of the intensity of the field inside the cavity, which justifies the use of the mean-field approximation. Under these conditions, Airy's equation (7.3.3) reduces to

$$A_2 = \frac{\tau A_1}{1 - R(1 - \alpha l)}. \tag{7.3.4}$$

The analogous equation relating the incident and circulating intensities $I_i = 2n\epsilon_0 |A_i|^2$ for $i = 1, 2$ is given by

$$I_2 = \frac{T I_1}{[1 - R(1 - \alpha l)]^2}. \tag{7.3.5}$$

This equation can be simplified by introducing the dimensionless parameter C (known as the cooperation number),

$$C = \frac{R\alpha l}{1 - R}, \tag{7.3.6}$$

which becomes (since $1 + C = (1 - R + R\alpha l)/(1 - R) = [1 - R(1 - \alpha l)]/T$)

$$I_2 = \frac{1}{T} \frac{I_1}{(1 + C)^2}. \tag{7.3.7}$$

We now assume that the absorption coefficient α and hence the parameter C depend on the intensity of the light within the interferometer. For simplicity, we assume that the absorption coefficient obeys the relation valid for a two-level saturable absorber,

$$\alpha = \frac{\alpha_0}{1 + I/I_s}, \tag{7.3.8}$$

where α_0 denotes the unsaturated absorption coefficient, I the local value of the intensity, and I_s the saturation intensity. For simplicity we also ignore the standing-wave nature of the field within the interferometer and take I equal to $I_2 + I_2' \approx 2I_2$. It is only approximately valid to ignore standing-wave effects for the interferometer of Fig. 7.3.1, but it is strictly valid for the traveling-wave interferometer shown in Fig. 7.3.2. Under the assumption that the absorption

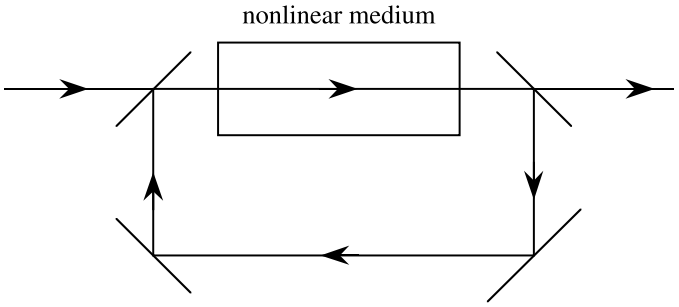

FIGURE 7.3.2: Bistable optical device in the form of a traveling wave interferometer containing a nonlinear medium.

coefficient depends on the intensity of the internal fields according to Eq. (7.3.8) with $I = 2I_2$, the parameter C is given by

$$C = \frac{C_0}{1 + 2I_2/I_s}, \tag{7.3.9}$$

with $C_0 = R\alpha_0 l/(1 - R)$. The relation between I_1 and I_2 given by Eq. (7.3.7) can be rewritten using this expression for C as

$$I_1 = TI_2\left(1 + \frac{C_0}{1 + 2I_2/I_s}\right)^2. \tag{7.3.10}$$

Finally, the output intensity I_3 is related to I_2 by

$$I_3 = TI_2. \tag{7.3.11}$$

The input–output relation implied by Eqs. (7.3.10) and (7.3.11) is illustrated graphically in Fig. 7.3.3 for several different values of the weak-field parameter C_0. For C_0 greater than 8, more than one output intensity can occur for certain values of the input intensity, which shows that the system possesses multiple solutions.

The input–output characteristics for a system showing optical bistability are shown schematically in Fig. 7.3.4(a). The portion of the curve that has a negative slope is shown by a dashed line. This portion corresponds to the branch of the solution to Eq. (7.3.10) for which the output intensity increases as the input intensity decreases. As might be expected on intuitive grounds, and as can be verified by means of a linear stability analysis, this branch of the solution is unstable; if the system is initially in this state, it will rapidly switch to one of the stable solutions through the growth of small perturbations.

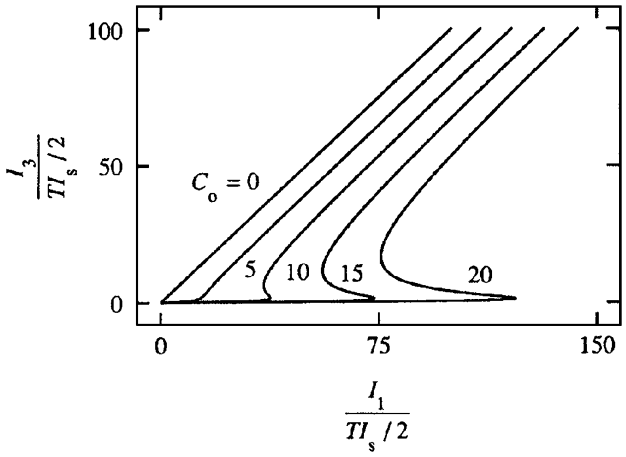

FIGURE 7.3.3: The input–output relation for a bistable optical device described by Eqs. (7.3.10) and (7.3.11).

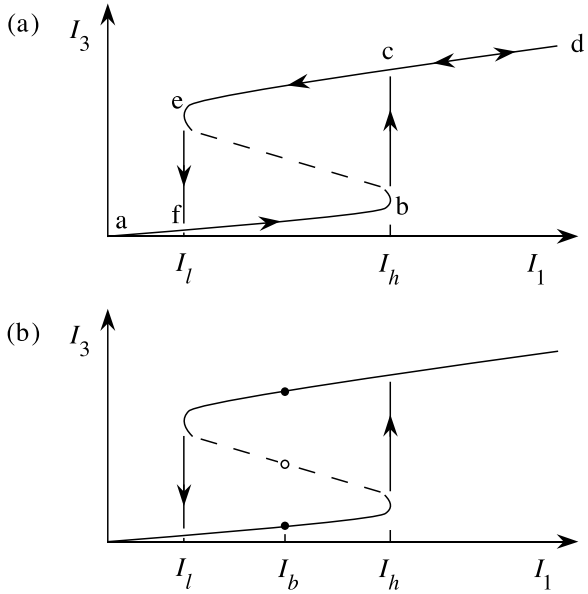

FIGURE 7.3.4: Schematic representation of the input–output characteristics of a system showing optical bistability.

The solution shown in Fig. 7.3.4(a) displays hysteresis in the following sense. We imagine that the input intensity I_1 is initially zero and is slowly increased. As I_1 is increased from zero to I_h (the high jump point), the output intensity is given by the *lower branch* of the solution—that

is, by the segment terminated by points a and b. As the input intensity is increased still further, the output intensity must jump to point c and trace out that portion of the curve labeled c–d. If the intensity is now slowly decreased, the system will remain on the upper branch and the output intensity will be given by the curve segment e–d. As the input intensity passes through the value I_l (the low jump point), the system makes a transition to point f and traces out the curve of f–a as the input intensity is decreased to zero.

The use of such a device as an optical switch is illustrated in part (b) of Fig. 7.3.4. If the input intensity is held fixed at the value I_b (the bias intensity), the two stable output points indicated by the filled dots are possible. The state of the system can be used to store binary information. The system can be forced to make a transition to the upper state by injecting a pulse of light so that the total input intensity exceeds I_h; the system can be forced to make a transition to the lower state by momentarily blocking the input beam.

7.3.2 Refractive Bistability

Let us now consider the case in which the absorption coefficient vanishes but in which the refractive index n depends nonlinearly on the optical intensity. For $\alpha = 0$, Eq. (7.3.3) becomes

$$A_2 = \frac{\tau A_1}{1 - \rho^2 e^{2ikl}} = \frac{\tau A_1}{1 - Re^{i\delta}}. \tag{7.3.12}$$

In obtaining the second form of this equation, we have written ρ^2 in terms of its amplitude and phase as

$$\rho^2 = Re^{i\phi} \tag{7.3.13}$$

and have introduced the total phase shift δ acquired in a round trip through the cavity. This phase shift is the sum

$$\delta = \delta_0 + \delta_2 \tag{7.3.14}$$

of a linear contribution

$$\delta_0 = \phi + 2n_0 \frac{\omega}{c} l \tag{7.3.15}$$

and a nonlinear contribution

$$\delta_2 = 2n_2 I \frac{\omega}{c} l, \tag{7.3.16}$$

where

$$I = I_2 + I_2' \simeq 2I_2. \tag{7.3.17}$$

Eq. (7.3.12) can be used to relate the intensities $I_i = 2n\epsilon_0 c|A_i|^2$ of the incident and internal fields as

$$\begin{aligned} I_2 &= \frac{TI_1}{(1 - Re^{i\delta})(1 - Re^{-i\delta})} = \frac{TI_1}{1 + R^2 - 2R\cos\delta} \\ &= \frac{TI_1}{(1 - R)^2 + 4R\sin^2\frac{1}{2}\delta} = \frac{TI_1}{T^2 + 4R\sin^2\frac{1}{2}\delta} \\ &= \frac{I_1/T}{1 + (4R/T^2)\sin^2\frac{1}{2}\delta}, \end{aligned} \tag{7.3.18}$$

which shows that

$$\frac{I_2}{I_1} = \frac{1/T}{1 + (4R/T^2)\sin^2\frac{1}{2}\delta}, \tag{7.3.19}$$

where, according to Eqs. (7.3.14) through (7.3.17), the phase shift is given by

$$\delta = \delta_0 + (4n_2\omega l/c)I_2. \tag{7.3.20}$$

In order to determine the conditions under which bistability can occur, we solve Eqs. (7.3.19) and (7.3.20) for the internal intensity I_2 as a function of the incident intensity I_1. This procedure is readily performed graphically by plotting each side of Eq. (7.3.19) as a function of I_2. Such a plot is shown in Fig. 7.3.5. We see that the system can possess one, three, five, or more solutions depending on the value of I_1. For the case in which three solutions exist for the range of input intensities I_1 that are available, a plot of I_3 versus I_1 looks very much like the curves shown in Fig. 7.3.4. Hence, the qualitative discussion of optical bistability given above is applicable in this case as well.

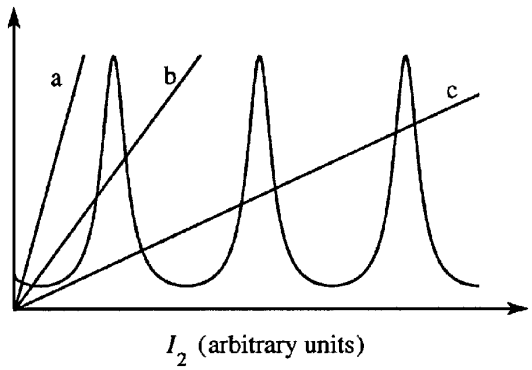

FIGURE 7.3.5: Graphical solution to Eq. (7.3.19). The oscillatory curve represents the right-hand side of this equation, and the straight lines labeled a through c represent the left-hand side for increasing values of the input intensity I_1.

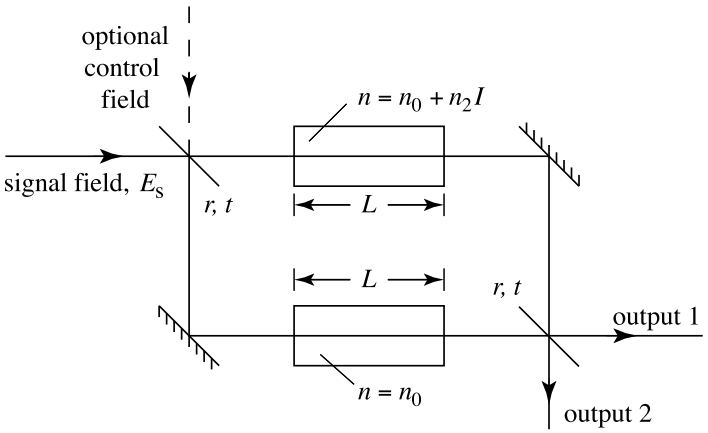

FIGURE 7.3.6: Configuration of an all-optical switch in the form of a Mach–Zehnder interferometer containing a nonlinear element. The input signal field is routed to either output 1 or 2 depending on its intensity and/or on the intensity of the control field.

More detailed treatments of optical bistability can be found in Lugiato (1984) and Gibbs (1985).

7.3.3 Optical Switching

Let us now analyze a prototypical all-optical switching device, as illustrated in Fig. 7.3.6. For simplicity, in the present analysis we assume that only a signal field is applied to the device; we shall show that this signal beam is directed to one or the other of the output ports depending on its intensity. Such an application of this device is illustrated in Fig. 7.3.7. A more general situation, in which both signal and control fields are applied to the device, can be treated by a similar but somewhat more detailed calculation, with the conclusion that the control field can be used to route the signal beam to either output port.

We assume that a signal field of amplitude E_s is incident upon the device and that the beam splitters are symmetric (have the same amplitude reflection and transmission coefficients r and t for beams incident on the beam splitter from either side) with coefficients given by*

$$r = i\sqrt{R}, \qquad t = \sqrt{T} \tag{7.3.21}$$

with

$$R + T = 1. \tag{7.3.22}$$

* This form of the beam-splitter relation ensures that the transfer characteristics obey a unitarity condition or equivalently that they obey the Stokes relations.

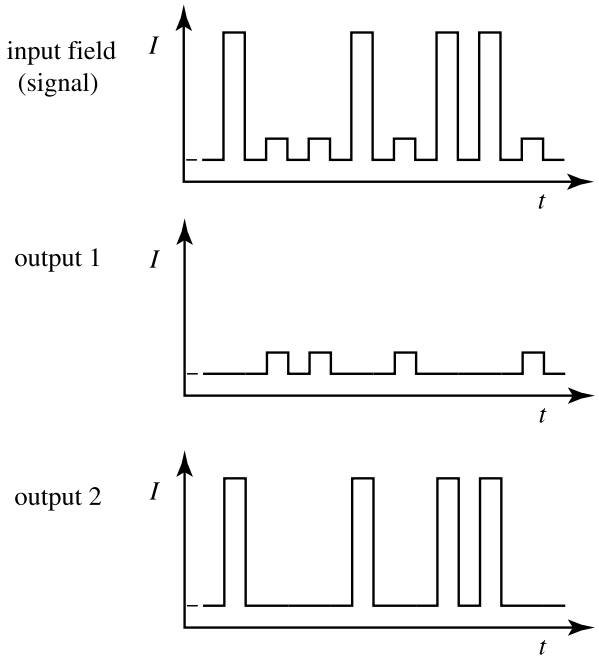

FIGURE 7.3.7: Illustration of the use of the device of Fig. 7.3.6 (without a control field) as a pulse sorter. The weaker pulses are routed to output 1, and the stronger pulses are routed to output 2.

The field at output port 1 is then seen to be given by

$$E_1 = E_s\left(rt + rte^{i\phi_{\rm NL}}\right), \tag{7.3.23}$$

where

$$\phi_{\rm NL} = n_2(\omega/c)IL = n_2(\omega/c)|t|^2(2n_0\epsilon_0 c)|E_s|^2 L. \tag{7.3.24}$$

The intensity at output port 1 is thus proportional to

$$\begin{aligned} |E_1|^2 &= |E_s|^2|r|^2|t|^2\left(1 + e^{i\phi_{\rm NL}}\right)\left(1 + e^{-i\phi_{\rm NL}}\right) \\ &= 2|E_s|^2 RT(1 + \cos\phi_{\rm NL}). \end{aligned} \tag{7.3.25}$$

We similarly find that the output at port 2 is given by

$$E_2 = E_s\left(r^2 + t^2 e^{i\phi_{\rm NL}}\right) \tag{7.3.26}$$

with an intensity proportional to

$$|E_2|^2 = |E_s|^2\left[R^2 + T^2 - 2RT\cos\phi_{\rm NL}\right]. \tag{7.3.27}$$

Note that

$$|E_1|^2 + |E_2|^2 = |E_s|^2 \tag{7.3.28}$$

as required by conservation of energy. These relations are illustrated in Fig. 7.3.8 and lead to the sort of behavior shown qualitatively in Fig. 7.3.7.

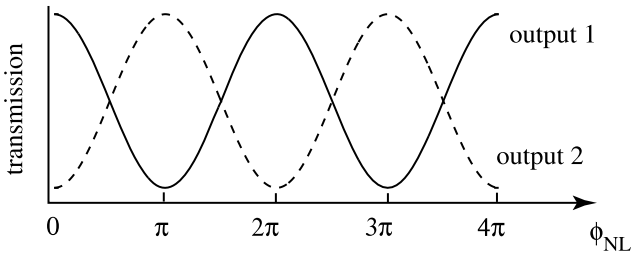

FIGURE 7.3.8: Plot of the transfer relations described by Eqs. (7.3.25) and (7.3.27).

Even though the calculation just presented is somewhat simplistic in that it considers the situation in which there is only a single input beam, it illustrates a crucial point: A nonlinear phase shift of π radians is required to produce high-contrast all-optical switching. The requirement that the nonlinear phase shift be as large as π radians is generic to a broad class of all-optical switching devices.

Let us therefore examine more carefully the conditions under which a nonlinear phase shift of π radians can be achieved. Let us first examine the consequences of using a nonlinear optical material that displays linear absorption. Under this circumstance the nonlinear phase shift is given by

$$\phi_{\mathrm{NL}} = n_2(\omega/c)\int_0^L I(z)\,dz, \tag{7.3.29}$$

where

$$I(z) = I_0 e^{-\alpha z}. \tag{7.3.30}$$

Straightforward integration leads to the result

$$\phi_{\mathrm{NL}} = n_2(\omega/c) I_0 L_{\mathrm{eff}}, \tag{7.3.31a}$$

where

$$L_{\mathrm{eff}} = \frac{1 - e^{-\alpha L}}{\alpha}. \tag{7.3.31b}$$

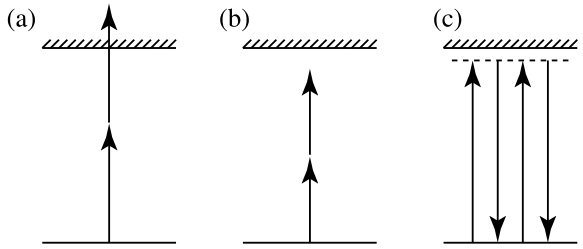

FIGURE 7.3.9: Two-photon absorption (shown in (a)) can be prevented by utilizing a material (b) such that the laser frequency lies below the half-band-gap energy. This strategy, however, precludes the use of one-photon-resonant nonlinearities (c).

Note that

$$L_{\text{eff}} \to L \qquad \text{for } \alpha L \ll 1, \tag{7.3.32a}$$

$$L_{\text{eff}} \to 1/\alpha \qquad \text{for } \alpha L \gg 1. \tag{7.3.32b}$$

Thus, for a strongly absorbing nonlinear optical material the effective interaction length can be much shorter than the physical length of the nonlinear medium. We also note that optical damage (see also Chapter 11) imposes a limit on how large a value of I_0 can be used for a particular material. Thus certain materials cannot even in principle be used for all-optical switching.

When the optical material displays two-photon absorption as well as linear absorption, the absorption coefficient appearing in Eq. (7.3.30) should be replaced by

$$\alpha = \alpha_0 + \beta I, \tag{7.3.33}$$

where β is the two-photon absorption coefficient.

Two-photon absorption is often a significant problem in the design of all-optical switching devices because it occurs at the same order of nonlinearity as the intensity-dependent refractive index n_2 (because these processes are proportional to the imaginary and real parts of $\chi^{(3)}$, respectively). Two-photon absorption can be eliminated entirely by choosing a material for which the lowest-lying excited state lies more than $2\hbar\omega$ above the ground state, as illustrated schematically in Fig. 7.3.9. A good summary of all-optical switching has been presented by Stegeman and Miller (1993).

7.4 Two-Beam Coupling

Let us consider the situation shown in Fig. 7.4.1 in which two beams of light (which in general have different frequencies) interact in a nonlinear material. Under certain conditions, the two

beams interact in such a manner that energy is transferred from one beam to the other; this phenomenon is known as two-beam coupling. Two-beam coupling is a process that is automatically phase-matched. Consequently the efficiency of the process does not depend critically upon the angle θ between the two beams. The reason why this process is automatically phase-matched will be clarified by the following analysis; for the present it is perhaps helpful to note that the origin of two-beam coupling is that the refractive index experienced by either wave is modified by the *intensity* of the other wave.

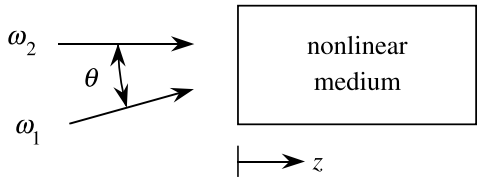

FIGURE 7.4.1: Two-beam coupling. We wish to determine the circumstances under which power can be transferred from the beam of frequency ω_1 to the beam of frequency ω_2.

Two-beam coupling occurs under several different circumstances in nonlinear optics. We saw in Chapter 6 that the nonlinear response of a two-level atom to pump and probe fields can lead to amplification of the probe wave. Furthermore, we shall see in Chapters 9 and 10 that gain occurs for various scattering processes such as stimulated Brillouin scattering and stimulated Raman scattering. Furthermore, in Chapter 11 we shall see that two-beam coupling occurs in many photorefractive materials. In the present section, we examine two-beam coupling from a general point of view that elucidates the conditions under which such energy transfer can occur. Our analysis is similar to that of Silberberg and Bar-Joseph (1982, 1984).

We describe the total optical field within the nonlinear medium as

$$\tilde{E}(\mathbf{r},t) = A_1 e^{i(\mathbf{k_1}\cdot\mathbf{r}-\omega_1 t)} + A_2 e^{i(\mathbf{k_2}\cdot\mathbf{r}-\omega_2 t)} + \text{c.c.}, \tag{7.4.1}$$

where $k_i = n_0\omega_i/c$, with n_0 denoting the linear part of the refractive index experienced by each wave. We now consider the intensity distribution associated with the interference between the two waves. The intensity is given in general by

$$I = n_0\epsilon_0 c\langle \tilde{E}^2 \rangle, \tag{7.4.2}$$

where the angular brackets denote an average over a time interval of many optical periods. The intensity distribution for $\tilde{E}$ given by Eq. (7.4.1) is hence given by

$$\begin{aligned} I &= 2n_0\epsilon_0 c\{A_1A_1^* + A_2A_2^* + [A_1A_2^* e^{i(\mathbf{k_1}-\mathbf{k_2})\cdot\mathbf{r}-i(\omega_1-\omega_2)t} + \text{c.c.}]\} \\ &= 2n_0\epsilon_0 c\{A_1A_1^* + A_2A_2^* + [A_1A_2^* e^{i(\mathbf{q}\cdot\mathbf{r}-\delta t)} + \text{c.c.}]\}, \end{aligned} \tag{7.4.3}$$

where in writing the second form we have introduced the wavevector difference (or "grating" wavevector)

$$\mathbf{q} = \mathbf{k_1} - \mathbf{k_2} \tag{7.4.4a}$$

and the frequency difference

$$\delta = \omega_1 - \omega_2. \tag{7.4.4b}$$

For the geometry of Fig. 7.4.1, the interference pattern has the form shown in Fig. 7.4.2, where we have assumed the condition $|\delta| \ll \omega_1$. Note that the pattern moves upward for $\delta > 0$, moves downward for $\delta < 0$, and is stationary for $\delta = 0$.

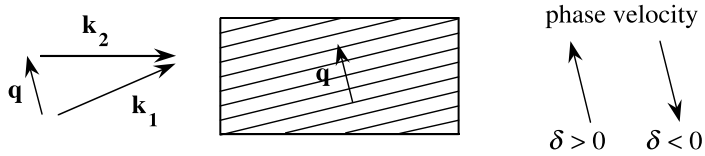

FIGURE 7.4.2: Interference pattern formed by two interacting waves.

A particularly simple example is the special case in which $\theta = 180°$. Then, again assuming that $|\delta| \ll \omega_1$, we find that the wavevector difference is given approximately by

$$\mathbf{q} \simeq -2\mathbf{k_2} \tag{7.4.5}$$

and thus that the intensity distribution is given by

$$I = 2n_0\epsilon_0 c\left\{A_1A_1^* + A_2A_2^* + \left[A_1A_2^* e^{i(-2kz-\delta t)} + \text{c.c.}\right]\right\}. \tag{7.4.6}$$

The interference pattern is hence of the form shown in Fig. 7.4.3. If δ is positive, the interference pattern moves to the left, and if δ is negative, it moves to the right—in either case with phase velocity $|\delta|/2k$.

Since the material system is nonlinear, a refractive index variation accompanies this intensity variation. Each wave is scattered by this index variation, or grating. We shall show below that no energy transfer accompanies this interaction for the case of a nonlinear material that responds instantaneously to the applied field. In order to allow the possibility of energy transfer, we assume that the nonlinear part of the refractive index (n_{NL}) obeys a Debye relaxation equation of the form

$$\tau \frac{dn_{\text{NL}}}{dt} + n_{\text{NL}} = n_2 I, \tag{7.4.7}$$

where τ is a measure of the response time of the material, that is, the characteristic time for the nonlinear response to develop. Note that this equation predicts that, in steady state, the

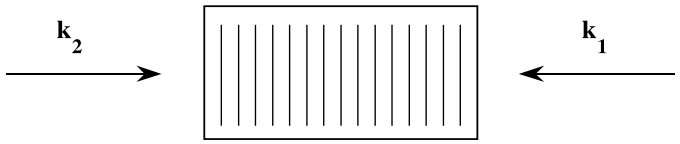

FIGURE 7.4.3: Interference pattern formed by two counterpropagating beams.

nonlinear contribution to the refractive index is given simply by $n_{\rm NL} = n_2 I$, in consistency with Eq. (4.1.15). However, under transient conditions it predicts that the nonlinearity develops in a time interval of the order of τ.

Eq. (7.4.7) can be solved (i.e., by the method of variation of parameters or by the Green's function method) to give the result

$$n_{\rm NL} = \frac{n_2}{\tau}\int_{-\infty}^{t} I(t')e^{(t'-t)/\tau}\,dt'. \tag{7.4.8}$$

The expression (7.4.3) for the intensity $I(t)$ is next introduced into this equation. We find, for example, that the part of $I(t)$ that varies as $e^{-i\delta t}$ leads to an integral of the form

$$\int_{-\infty}^{t} e^{-i\delta t'}e^{(t'-t)/\tau}\,dt' = e^{-t/\tau}\int_{-\infty}^{t} e^{(-i\delta+1/\tau)t'}\,dt' = \frac{e^{-i\delta t}}{-i\delta+1/\tau}, \tag{7.4.9}$$

with a similar result for the part of $I(t)$ that varies as $e^{i\delta t}$. Eq. (7.4.8) hence shows that the nonlinear contribution to the refractive index is given by

$$n_{\rm NL} = 2n_0 n_2 \epsilon_0 c\left[\left(A_1A_1^* + A_2A_2^*\right) + \frac{A_1A_2^* e^{i(\mathbf{q}\cdot\mathbf{r}-\delta t)}}{1-i\delta\tau} + \frac{A_1^*A_2 e^{-i(\mathbf{q}\cdot\mathbf{r}-\delta t)}}{1+i\delta\tau}\right]. \tag{7.4.10}$$

Because of the complex nature of the denominators, the refractive index variation is not in general in phase with the intensity distribution.

In order to determine the degree of coupling between the two fields, we require that the field given by Eq. (7.4.1) satisfy the wave equation

$$\nabla^2\tilde{E} - \frac{n^2}{c^2}\frac{\partial^2\tilde{E}}{\partial t^2} = 0, \tag{7.4.11}$$

where we take the refractive index to have the form

$$n = n_0 + n_{\rm NL}. \tag{7.4.12}$$

We make the physical assumption that $|n_{\rm NL}| \ll n_0$, in which case it is a good approximation to express n^2 as

$$n^2 = n_0^2 + 2n_0 n_{\rm NL}. \tag{7.4.13}$$

Let us consider the part of Eq. (7.4.11) that shows a spatial and temporal dependence given by $\exp[i(\mathbf{k_2}\cdot\mathbf{r}-\omega_2 t)]$. Using Eqs. (7.4.1), (7.4.10), and (7.4.13), we find that this portion of Eq. (7.4.11) is given by

$$\frac{d^2A_2}{dz^2}+2ik_2\frac{dA_2}{dz}-k_2^2A_2+\frac{n_0^2\omega_2^2}{c^2}A_2 = -\frac{4n_0^2n_2\omega_2^2\epsilon_0}{c}\left(|A_1|^2+|A_2|^2\right)A_2-\frac{4n_0^2n_2\omega_1^2\epsilon_0}{c}\frac{|A_1|^2A_2}{1+i\delta\tau}. \tag{7.4.14}$$

Note that the origin of the last term on the right-hand side is the scattering of the field $A_1\exp[i(\mathbf{k_1}\cdot\mathbf{r}-\omega_1 t)]$ from the time-varying refractive index distribution (i.e., the moving grating)

$$(2n_0\epsilon_0n_2c)A_1^*A_2\frac{e^{-i(\mathbf{q}\cdot\mathbf{r}-\delta t)}}{1+i\delta\tau},$$

whereas the origin of the first term on the right-hand side is the scattering of the field $A_2\exp[i(\mathbf{k_2}\cdot\mathbf{r}-\omega_2 t)]$ from the stationary refractive index variation

$$(2n_0\epsilon_0n_2c)\left(A_1A_1^*+A_2A_2^*\right).$$

We next drop the first term on the left-hand side of Eq. (7.4.14) by making the slowly varying amplitude approximation, and we note that the third and fourth terms exactly cancel. The equation then reduces to

$$\frac{dA_2}{dz}=2in_0n_2(\omega/c)\left[\left(|A_1|^2+|A_2|^2\right)A_2+\frac{|A_1|^2A_2}{1+i\delta\tau}\right], \tag{7.4.15}$$

where, to good approximation, we have replaced ω_1 and ω_2 by ω. We now calculate the rate of change of intensity of the ω_2 field. We introduce the intensities

$$I_1=2n_0\epsilon_0cA_1A_1^* \quad \text{and} \quad I_2=2n_0\epsilon_0cA_2A_2^* \tag{7.4.16}$$

and note that the spatial variation of I_2 is given by

$$\frac{dI_2}{dz}=2n_0\epsilon_0c\left(A_2^*\frac{dA_2}{dz}+A_2\frac{dA_2^*}{dz}\right). \tag{7.4.17}$$

We then find from Eqs. (7.4.15) through (7.4.17) that

$$\frac{dI_2}{dz}=\frac{2n_2\omega}{c}\frac{\delta\tau}{1+\delta^2\tau^2}I_1I_2. \tag{7.4.18}$$

Note that only the last term on the right-hand side of Eq. (7.4.15) contributes to energy transfer. The frequency dependence of the right-hand side of Eq. (7.4.18) is shown in Fig. 7.4.4.

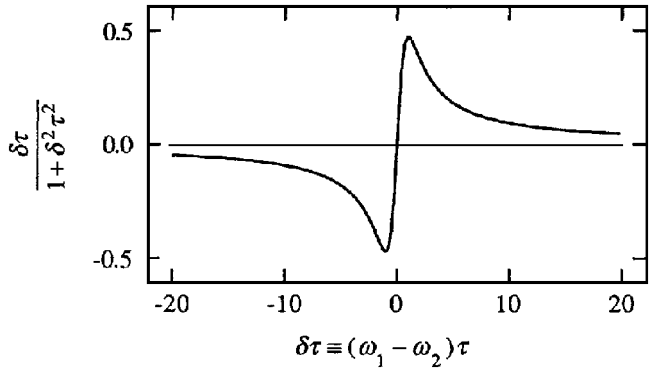

FIGURE 7.4.4: Frequency dependence of the gain for two-beam coupling.

For the case of a positive value of n_2 (e.g., for the molecular orientation Kerr effect, for electrostriction, for a two-level atom with the optical frequencies above the resonance frequency), Eq. (7.4.18) predicts gain for positive δ, that is, for $\omega_2 < \omega_1$. Conversely, when n_2 is negative, this equation predicts that the higher-frequency wave will be amplified at the expense of the lower frequency wave. For the case of n_2 positive, the excess photon energy is transferred to the thermal reservoir associated with the material medium; for n_2 negative, energy is extracted from this thermal reservoir. We note that the extraction of energy from a thermal reservoir plays a crucial role in the process of laser cooling of atoms.

Note that the ω_2 wave experiences maximum gain (for n_2 positive) for $\delta\tau = 1$, in which case Eq. (7.4.18) becomes

$$\frac{dI_2}{dz} = n_2 \frac{\omega}{c} I_1 I_2. \tag{7.4.19}$$

Note also from Eq. (7.4.18) that in the limit of an infinitely fast nonlinearity, that is, in the limit $\tau \to 0$, the coupling of intensity between the two waves vanishes. The reason for this behavior is that only the imaginary part of the (total) refractive index can lead to a change in intensity of the ω_2 wave. We see from Eq. (7.4.10) that (for n_2 real, as has been assumed throughout this discussion) the only way in which n_{NL} can become complex is for τ to be nonzero. When τ is nonzero, the response can lag in phase behind the driving term, leading to a complex value of the nonlinear contribution to the refractive index.

The theory just presented predicts that there will be no energy coupling if the product $\delta\tau$ vanishes, either because the nonlinearity has a fast response or because the input waves are at the same frequency. However, two-beam coupling can occur in certain photorefractive crystals even between beams of the same frequency (Feinberg, 1983). In such cases, energy transfer occurs as a result of a *spatial* phase shift between the nonlinear index grating and the optical intensity distribution. The direction of energy flow depends upon the orientation of the

wavevectors of the optical beams with respect to some symmetry axis of the photorefractive crystal. The photorefractive effect is described in greater detail in Chapter 11.

7.5 Pulse Propagation and Temporal Solitons

In this section we study some of the nonlinear optical effects that can occur when short optical pulses propagate through dispersive nonlinear optical media. We shall see that the spectral content of the pulse can become modified by the nonlinear optical process of self-phase modulation. This process is especially important for pulses of high peak intensity. We shall also see that (even for the case of a medium with a linear response) the shape of the pulse can become modified by means of propagation effects such as dispersion of the group velocity within the medium. This process is especially important for very short optical pulses, which necessarily have a broad spectrum. In general, self-phase modulation and group-velocity dispersion occur simultaneously, and both tend to modify the shape of the optical pulse. However, under certain circumstances, which are described below, an exact cancellation of these two effects can occur, allowing a special type of pulse known as a temporal optical soliton to propagate through large distances with no change in pulse shape.

7.5.1 Self-Phase Modulation

Self-phase modulation is the change in the phase of an optical pulse resulting from the nonlinearity of the refractive index of the material medium. In order to understand the origin of this effect, let us consider the propagation of the optical pulse

$$\tilde{E}(z,t) = \tilde{A}(z,t)e^{i(k_0 z - \omega_0 t)} + \text{c.c.} \tag{7.5.1}$$

through a medium characterized by a nonlinear refractive index of the sort

$$n(t) = n_0 + n_2 I(t), \tag{7.5.2}$$

where $I(t) = 2n_0\epsilon_0 c|\tilde{A}(z,t)|^2$. Note that for the present we are assuming that the medium can respond essentially instantaneously to the pulse intensity. We also assume that the length of the nonlinear medium is sufficiently small that no reshaping of the optical pulse can occur within the medium; the only effect of the medium is to change the phase of the transmitted pulse by the amount

$$\phi_{\text{NL}}(t) = -n_2 I(t)\omega_0 L/c. \tag{7.5.3}$$

As a result of the time-varying phase of the wave, the spectrum of the transmitted pulse will be modified and typically will be broader than that of the incident pulse. From a formal point

of view, we can determine the spectral content of the transmitted pulse by calculating its energy spectrum

$$S(\omega) = \left| \int_{-\infty}^{\infty} \tilde{A}(t) e^{-i\omega_0 t - i\phi_{\mathrm{NL}}(t)} e^{i\omega t}\, dt \right|^2. \tag{7.5.4}$$

Self-phase modulation was studied initially by Brewer (1967), Shimizu (1967), and Cheung et al. (1968).

We shall return later in this section to an examination of the structure of Eq. (7.5.4). However, let us first develop an intuitive picture of the nature of the modification of the spectral content of the transmitted pulse by introducing the concept of the instantaneous frequency $\omega(t)$ of the pulse, which is given by

$$\omega(t) = \omega_0 + \delta\omega(t), \tag{7.5.5a}$$

where

$$\delta\omega(t) = \frac{d}{dt}\phi_{\mathrm{NL}}(t) \tag{7.5.5b}$$

denotes the variation of the instantaneous frequency. The instantaneous frequency is a well-defined concept and is given by Eqs. (7.5.5) whenever the amplitude $\tilde{A}(t)$ varies slowly compared to an optical period.

As an example of the use of these formulas, we consider the case illustrated in part (a) of Fig. 7.5.1, in which the pulse shape is given by the form

$$I(t) = I_0 \operatorname{sech}^2(t/\tau_0). \tag{7.5.6}$$

We then find from Eq. (7.5.3) that the nonlinear phase shift is given by

$$\phi_{\mathrm{NL}}(t) = -n_2 \frac{\omega_0}{c} L I_0 \operatorname{sech}^2(t/\tau_0), \tag{7.5.7}$$

and from Eq. (7.5.5b) that the change in instantaneous frequency is given by

$$\delta\omega(t) = 2n_2 \frac{\omega_0}{c\tau_0} L I_0 \operatorname{sech}^2(t/\tau_0) \tanh(t/\tau_0). \tag{7.5.8}$$

The variation in the instantaneous frequency is illustrated in part (b) of Fig. 7.5.1, under the assumption that n_2 is positive. We see that the leading edge of the pulse is shifted to lower frequencies and that the trailing edge is shifted to higher frequencies. This conclusion is summarized schematically in part (c) of the figure. The maximum value of the frequency shift is given by

$$\delta\omega_{\max} = \frac{-0.77\Delta\phi_{\mathrm{NL}}^{(\max)}}{\tau_0} \quad \text{where} \quad \Delta\phi_{\mathrm{NL}}^{(\max)} = -n_2 \frac{\omega_0}{c} I_0 L. \tag{7.5.9}$$

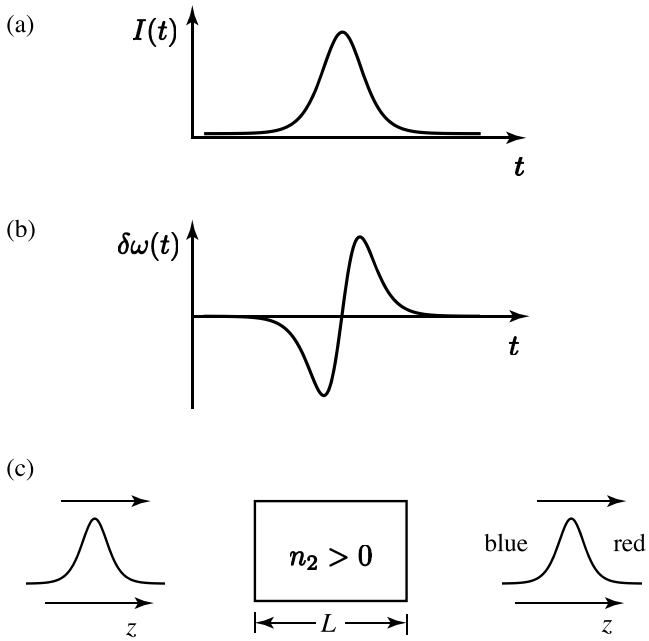

FIGURE 7.5.1: (a) Time dependence of the incident pulse. (b) Change in instantaneous frequency of the transmitted pulse. (c) Laboratory arrangement to observe self-phase modulation.

We expect that spectral broadening due to self-phase modulation will be very important whenever $\delta\omega_{\max}$ exceeds the spectral width of the incident pulse, which for the case of a smooth pulse is of the order of $1/\tau_0$. We thus expect self-phase modulation to be important whenever $\Delta\phi_{\mathrm{NL}}^{(\max)} \geq 2\pi$.

Let use now turn to an examination of form of Eq. (7.5.4); we make use of a procedure described by Shen and Yang (2006). We shall see that the nature of the resulting modification of the spectrum of the transmitted pulse provides a convenient means for the measurement of nonlinear optical coefficients such as n_2, as implemented by Kim et al. (1994). We assume that $\phi_{\mathrm{NL}}(t)$ has a shape that is a Gaussian in time, and that as above the instantaneous frequency shift is given by $d\phi_{\mathrm{NL}}/dt$. Except at the points of inflection of the Gaussian function, there will be two contributions to the integral in Eq. (7.5.4) that give the same frequency shift. These contributions will add either constructively or destructively depending on the relative phases of these contributions. We take $\phi_{\mathrm{NL}}^{\max}$ to represent the maximum value of the nonlinear phase shift experienced upon propagation through the nonlinear medium. The total number of interference peaks is then expected to be equal to $\phi_{\mathrm{NL}}^{\max}/2\pi$. We further expect that the spectrum will be broadened to a total width of $\Delta\omega = \phi_{\mathrm{NL}}^{\max}/T$ where T is a measure of the pulse duration. An example of such behavior is shown in Fig. 7.5.2, which was obtained by direct numerical integration of Eq. (7.5.4).

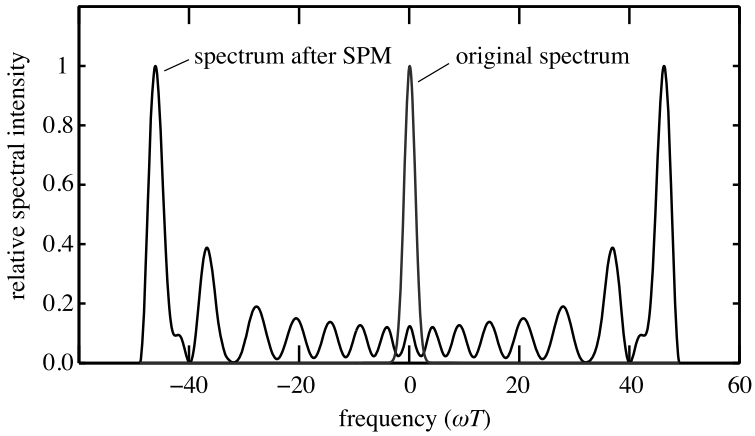

FIGURE 7.5.2: Modification of a laser pulse spectrum by the process of self-phase modulation (SPM). For this example, the input pulse was assumed to possess a Gaussian time evolution with a peak intensity chosen to produce $\phi_{\mathrm{NL}}^{\max} = 30\pi$ radians of nonlinear phase shift. The pulse half width to the e^{-2} intensity point is take to be T. We see that the spectral width is equal to $30\pi \simeq 100$ in the dimensionless units of the plot and that the number of peaks is equal to $\phi_{\mathrm{NL}}^{\max}/2\pi = 15$, in agreement with the simple model presented in the text.

7.5.2 Pulse Propagation Equation

Let us next consider the equations that govern the propagation of the pulse

$$\tilde{E}(z,t) = \tilde{A}(z,t)e^{i(k_0 z - \omega_0 t)} + \text{c.c.}, \tag{7.5.10}$$

where $k_0 = n_{\mathrm{lin}}(\omega_0)\omega_0/c$, through a dispersive, nonlinear optical medium. In particular, we seek an equation that describes how the pulse envelope function $\tilde{A}(z,t)$ propagates through the medium. We begin with the wave equation in the form (see also Eq. (2.1.9a))

$$\frac{\partial^2 \tilde{E}}{\partial z^2} - \frac{1}{\epsilon_0 c^2}\frac{\partial^2 \tilde{D}}{\partial t^2} = 0, \tag{7.5.11}$$

where $\tilde{D}$ represents the total displacement field, including both linear and nonlinear contributions. We now introduce the Fourier transforms $\tilde{E}(z,t)$ and $\tilde{D}(z,t)$ by means of the equations

$$\tilde{E}(z,t) = \int_{-\infty}^{\infty} E(z,\omega)e^{-i\omega t}\frac{d\omega}{2\pi}, \qquad \tilde{D}(z,t) = \int_{-\infty}^{\infty} D(z,\omega)e^{-i\omega t}\frac{d\omega}{2\pi}. \tag{7.5.12}$$

The Fourier amplitudes $E(z,\omega)$ and $D(z,\omega)$ are related by

$$D(z,\omega) = \epsilon_0 \epsilon(\omega) E(z,\omega), \tag{7.5.13}$$

where $\epsilon(\omega)$ is the effective dielectric constant that describes both the linear and nonlinear contributions to the response.

Eqs. (7.5.12) and (7.5.13) are now introduced into the wave equation (7.5.11), which leads to the result that each Fourier component of the field must obey the equation

$$\frac{\partial^2 E(z,\omega)}{\partial z^2} + \epsilon(\omega)\frac{\omega^2}{c^2} E(z,\omega) = 0. \tag{7.5.14}$$

This frequency-domain form of the wave equation is known as a Helmholtz equation.

We now write this equation in terms of the Fourier transform of $\tilde{A}(z,t)$, which is given by

$$A(z,\omega') = \int_{-\infty}^{\infty} \tilde{A}(z,t) e^{i\omega' t}\, dt. \tag{7.5.15}$$

Here we represent the transform variable as ω' rather than as ω to emphasize the fact that the frequency content of $\tilde{A}(z,t)$ does not extend to optical frequencies. We next need to relate $A(z,\omega')$ to $E(z,\omega)$, because it is the latter quantity that appears in the frequency-domain wave equation (7.5.14). We express $E(z,\omega)$ as

$$\begin{aligned} E(z,\omega) &= \int_{-\infty}^{\infty} \tilde{E}(z,t) e^{i\omega t} dt \\ &= \int_{-\infty}^{\infty} \tilde{A}(z,t) e^{ik_0 z} e^{i(\omega-\omega_0)t} dt + \int_{-\infty}^{\infty} \tilde{A}^*(z,t) e^{-ik_0 z} e^{i(\omega+\omega_0)t} dt \end{aligned}$$

and which can be expressed as

$$\begin{aligned} E(z,\omega) &= A(z,\omega-\omega_0) e^{ik_0 z} + A^*(z,\omega+\omega_0) e^{-ik_0 z} \\ &\simeq A(z,\omega-\omega_0) e^{ik_0 z}. \end{aligned} \tag{7.5.16}$$

Here the second, approximate, form is obtained by noting that a quantity such as $\tilde{A}(z,t)$ that varies slowly in time cannot possess high-frequency Fourier components. This expression for $E(z,\omega)$ is now introduced into Eq. (7.5.14), and the slowly-varying amplitude approximation is made so that the term containing $\partial^2 A/\partial z^2$ can be dropped. One obtains

$$2ik_0 \frac{\partial A(z,\omega-\omega_0)}{\partial z} + \left(k^2 - k_0^2\right) A(z,\omega-\omega_0) = 0, \tag{7.5.17}$$

where

$$k(\omega) = \sqrt{\epsilon(\omega)}\, \omega/c. \tag{7.5.18}$$

In practice, k typically differs from k_0 by only a small fractional amount, and thus to good approximation $k^2 - k_0^2$ can be replaced by $2k_0(k - k_0)$ so that Eq. (7.5.17) becomes

$$\frac{\partial A(z, \omega - \omega_0)}{\partial z} - i(k - k_0)A(z, \omega - \omega_0) = 0. \tag{7.5.19}$$

Recall that the propagation constant k depends both on the frequency and (through the intensity dependence of ϵ) on the intensity of the optical wave. It is often adequate to describe this dependence in terms of a truncated power series expansion of the form

$$k = k_0 + \Delta k_{\mathrm{NL}} + k_1(\omega - \omega_0) + \tfrac{1}{2}k_2(\omega - \omega_0)^2, \tag{7.5.20}$$

where, as before, $k_0 = n_{\mathrm{lin}}(\omega_0)/c$. In this expression, we have introduced the nonlinear contribution to the propagation constant given by

$$\Delta k_{\mathrm{NL}} = \Delta n_{\mathrm{NL}}\omega_0/c \tag{7.5.21}$$

and have introduced the quantities

$$k_1 = \left(\frac{dk}{d\omega}\right)_{\omega=\omega_0} = \frac{d}{d\omega}\left[\frac{n_{\mathrm{lin}}(\omega)\omega}{c}\right]_{\omega=\omega_0} = \frac{1}{c}\left[n_{\mathrm{lin}}(\omega) + \omega\frac{dn_{\mathrm{lin}}(\omega)}{d\omega}\right]_{\omega=\omega_0} \equiv \frac{n_g}{c} \equiv \frac{1}{v_g(\omega_0)} \tag{7.5.22}$$

and

$$k_2 = \left(\frac{d^2k}{d\omega^2}\right)_{\omega=\omega_0} = \frac{d}{d\omega}\left[\frac{1}{v_g(\omega)}\right]_{\omega=\omega_0} = \left(-\frac{1}{v_g^2}\frac{dv_g}{d\omega}\right)_{\omega=\omega_0}. \tag{7.5.23}$$

Here k_1 is the reciprocal of the group velocity $v_g = c/n_g$, where n_g is the group index, and where k_2 is a measure of the dispersion of the group velocity. It is routinely known as the group velocity dispersion (GVD) parameter.* As illustrated in Fig. 7.5.3, the long-wavelength components of an optical pulse propagate faster than the short-wavelength components when the group velocity dispersion parameter k_2 is positive, and travel more slowly when k_2 is negative.

* In the field of guided-wave photonics, k_2 is often denoted as β_2. Also, in many circumstances it is useful to describe GVD in terms of wavelength units rather than frequency units. This GVD parameter is defined as $D_\lambda = (d/d\lambda)(1/v_g)$, where by convention λ is the vacuum wavelength of the light given by the standard relation $\omega = 2\pi c/\lambda$. One then finds from straightforward differentiation that $D_\lambda = (-2\pi c/\lambda^2)k_2$. One can express the GVD parameter D_λ in terms of the refractive index as $D_\lambda = (d/d\lambda)(1/v_g) = (d/d\lambda)(n_g/c) = (d/d\lambda)(n - \lambda dn/d\lambda) = -(\lambda/c)(d^2n/d\lambda^2)$. For fused silica, $D_\lambda = 35\ \mathrm{fs}^2/\mathrm{mm}$ at 800 nm and $D_\lambda = -26\ \mathrm{fs}^2/\mathrm{mm}$ at 1500 nm. D_λ vanishes at a wavelength of approximately 1300 nm.

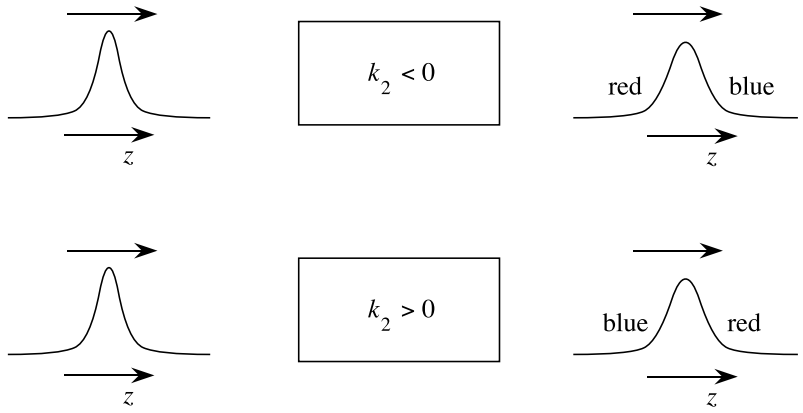

FIGURE 7.5.3: Pulse spreading resulting from group velocity dispersion.

The expression (7.5.20) for k is next introduced into the reduced wave equation (7.5.19), which becomes

$$\left[\frac{\partial}{\partial z} - i\,\Delta k_{\mathrm{NL}} - ik_1(\omega-\omega_0) - \tfrac{1}{2}ik_2(\omega-\omega_0)^2\right] A(z,\omega-\omega_0) = 0. \tag{7.5.24}$$

This equation is now transformed from the frequency domain to the time domain. To do so, we multiply each term by the factor $\exp[-i(\omega-\omega_0)t]$ and integrate the resulting equation over all values of $\omega-\omega_0$. We next evaluate the resulting integrals. First, by the definition of the Fourier transform, we find that

$$\int_{-\infty}^{\infty} A(z,\omega-\omega_0)e^{-i(\omega-\omega_0)t}\,\frac{d(\omega-\omega_0)}{2\pi} = \tilde{A}(z,t). \tag{7.5.25a}$$

Next, by formal differentiation with respect to the time variable, we find that

$$\begin{aligned}&\int_{-\infty}^{\infty}(\omega-\omega_0)A(z,\omega-\omega_0)e^{-i(\omega-\omega_0)t}\,\frac{d(\omega-\omega_0)}{2\pi}\\ &\quad= \frac{1}{-i}\frac{\partial}{\partial t}\int_{-\infty}^{\infty} A(z,\omega-\omega_0)e^{-i(\omega-\omega_0)t}\,\frac{d(\omega-\omega_0)}{2\pi} = i\frac{\partial}{\partial t}\tilde{A}(z,t),\end{aligned} \tag{7.5.25b}$$

and similarly that

$$\int_{-\infty}^{\infty}(\omega-\omega_0)^2A(z,\omega-\omega_0)e^{-i(\omega-\omega_0)t}\,\frac{d(\omega-\omega_0)}{2\pi} = -\frac{\partial^2}{\partial t^2}\tilde{A}(z,t). \tag{7.5.25c}$$

Eq. (7.5.24) then becomes

$$\frac{\partial\tilde{A}}{\partial z} + k_1\frac{\partial\tilde{A}}{\partial t} + \tfrac{1}{2}ik_2\frac{\partial^2\tilde{A}}{\partial t^2} - i\,\Delta k_{\mathrm{NL}}\tilde{A} = 0. \tag{7.5.26}$$

This equation can be simplified by means of a coordinate transformation. In particular, we introduce the retarded time τ by the substitution

$$\tau = t - \frac{z}{v_g} = t - k_1 z, \tag{7.5.27}$$

and we describe the optical pulse by the function $\tilde{A}_s(z, \tau)$, which is related to the function $\tilde{A}(z, t)$ by

$$\tilde{A}_s(z, \tau) = \tilde{A}(z, t). \tag{7.5.28}$$

We next use the chain rule of differentiation to establish that

$$\frac{\partial \tilde{A}}{\partial z} = \frac{\partial \tilde{A}_s}{\partial z} + \frac{\partial \tilde{A}_s}{\partial \tau}\frac{\partial \tau}{\partial z} = \frac{\partial \tilde{A}_s}{\partial z} - k_1 \frac{\partial \tilde{A}_s}{\partial \tau}, \tag{7.5.29a}$$

$$\frac{\partial \tilde{A}}{\partial t} = \frac{\partial \tilde{A}_s}{\partial z}\frac{\partial z}{\partial t} + \frac{\partial \tilde{A}_s}{\partial \tau}\frac{\partial \tau}{\partial t} = \frac{\partial \tilde{A}_s}{\partial \tau}, \tag{7.5.29b}$$

and analogously that $\partial^2 \tilde{A}/\partial t^2 = \partial^2 \tilde{A}_s/\partial \tau^2$. These expressions are now introduced into Eq. (7.5.26), which becomes

$$\frac{\partial \tilde{A}_s(z, \tau)}{\partial z} + \tfrac{1}{2} i k_2 \frac{\partial^2 \tilde{A}_s(z, \tau)}{\partial \tau^2} - i \Delta k_{\mathrm{NL}} \tilde{A}_s(z, \tau) = 0. \tag{7.5.30}$$

Finally, we express the nonlinear contribution to the propagation constant as

$$\Delta k_{\mathrm{NL}} = n_2 \frac{\omega_0}{c} I = 2 n_0 \epsilon_0 n_2 \omega_0 |\tilde{A}_s(z, \tau)|^2 \equiv \gamma |\tilde{A}_s(z, \tau)|^2, \tag{7.5.31}$$

so that Eq. (7.5.30) can be expressed as

$$\frac{\partial \tilde{A}_s(z, \tau)}{\partial z} + \tfrac{1}{2} i k_2 \frac{\partial^2 \tilde{A}_s(z, \tau)}{\partial \tau^2} = i \gamma |\tilde{A}_s(z, \tau)|^2 \tilde{A}_s(z, \tau). \tag{7.5.32}$$

This equation describes the propagation of optical pulses through dispersive, nonlinear optical media. Note that the second term on the left-hand side shows how pulses tend to broaden in time because of group velocity dispersion, and that the term on the right-hand side shows how pulses tend to broaden in frequency because of self-phase modulation. Eq. (7.5.32) is sometimes referred to as the nonlinear Schrödinger equation.

7.5.3 Temporal Optical Solitons

Note from the form of the pulse propagation equation (7.5.32) that it is possible for the effects of group velocity dispersion to compensate for the effects of self-phase modulation. In fact, under

appropriate circumstances the degree of compensation can be complete, and optical pulses can propagate through a dispersive, nonlinear optical medium with an invariant shape. Such pulses are known as temporal optical solitons.

As an example of a temporal optical soliton, note that Eq. (7.5.32) is satisfied identically by a pulse whose amplitude is of the form

$$\tilde{A}_s(z,\tau) = A_s^0 \operatorname{sech}(\tau/\tau_0) e^{i\kappa z}, \tag{7.5.33a}$$

where the pulse amplitude A_s^0 and pulse width τ_0 must be related according to

$$|A_s^0|^2 = \frac{-k_2}{\gamma \tau_0^2} = \frac{-k_2}{2n_0 \epsilon_0 n_2 \omega_0 \tau_0^2} \tag{7.5.33b}$$

and where

$$\kappa = -k_2/2\tau_0^2 = \tfrac{1}{2}\gamma |A_s^0|^2 \tag{7.5.33c}$$

represents the phase shift experienced by the pulse on propagation. One can verify by direct substitution that Eqs. (7.5.33) do in fact satisfy the pulse propagation equation (7.5.32) (see Problem 16 at the end of this chapter).

Note that condition (7.5.33b) shows that k_2 and n_2 must have opposite signs in order for Eq. (7.5.33a) to represent a physical pulse in which the intensity $|A_s^0|^2$ and the square of the pulse width τ_0^2 are both positive.

We can understand this result by referring back to the pulse propagation equation (7.5.32). Only if k_2 and n_2 have opposite signs can the second term on the left cancel the term on the right. In reaching this conclusion we should note that the term $\partial^2 \tilde{A}_s / \partial \tau^2$ will be negative near the peak of the pulse, where the contribution $i\gamma |\tilde{A}_s|^2 \tilde{A}_s$ is most important.

Expressions (7.5.33) give what is known as the fundamental soliton solution to the pulse propagation equation (7.5.32). Higher-order soliton solutions also are known. These solutions were first obtained through use of inverse scattering methods by Zakharov and Shabat (1972) and are described in more detail by Agrawal (1989).

One circumstance under which k_2 and γ have opposite signs occurs in fused-silica optical fibers. In this case, the nonlinearity in the refractive index occurs as the result of electronic polarization, and n_2 is consequently positive. The group velocity dispersion parameter k_2 is positive for visible light but becomes negative for wavelengths longer than approximately 1.3 μm. This effect is illustrated in Fig. 7.5.4, in which the linear refractive index n_{lin} and the group index $n_g \equiv c/v_g$ are plotted as functions of the vacuum wavelength of the incident radiation. Optical solitons of the sort described by Eq. (7.5.33a) have been observed by Mollenauer et al. (1980) in the propagation of light pulses at a wavelength of 1.55 μm obtained from a color center laser.

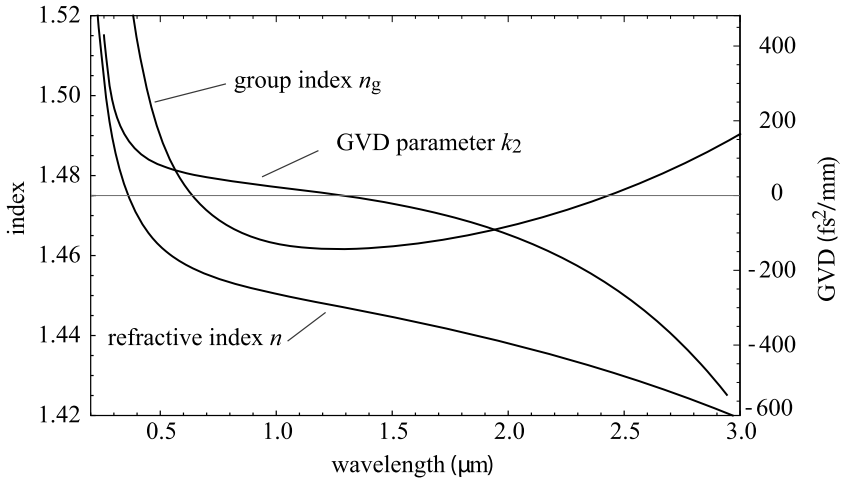

FIGURE 7.5.4: Dependence of the linear refractive index n, group index $n_g = c/v_g$, and the GVD parameter k_2 on the vacuum wavelength for fused silica.

Problems

1. *Spatial solitons.* Verify that Eqs. (7.1.19) through (7.1.21) do indeed satisfy Eq. (7.1.18).
2. *Self-focusing and beam breakup.* Read carefully the subsection that includes Eqs. (7.1.42) through (7.1.44) and write a short essay (one or two paragraphs) describing how you would proceed to observe beam breakup in the laboratory making use of a laser pulse of 10 nsec duration (assumed for simplicity to have a square-top time evolution) and making use of the nonlinear response of carbon disulfide. Describe issues such as the pulse energy that is required, the length of the interaction region you would use, and the focusing characteristics of your laser beam.
3. *Z-scan.* In this problem we develop a mathematical description of the Z-scan procedure for measuring the nonlinear refractive index. The basis of this procedure is that a sample is translated longitudinally through the beam-waist region of a focused gaussian laser beam, and the variation of the on-axis intensity in the far field is measured as a function of sample position. The on-axis intensity in the far field is usually determined by measuring the power transmitted through a small aperture placed on the system axis. The variation of measured power with sample position is found to be proportional to the nonlinear phase shift experienced in passing through the sample, and from this measured phase shift the value of n_2 of the sample can be determined from the known sample thickness L and laser intensity at the sample.

   In detail, you are to derive an expression for the dependence of the fractional change in on-axis intensity $\Delta I/I$ on the sample position z relative to the position z_0 of the beam

waist of the incident laser beam. This expression will also depend on the values of n_2, of L, and on the parameters of the incident laser beam. For simplicity, assume that the sample is thin both in the sense that L is much smaller than the confocal parameter b of the incident laser beam and in that the maximum nonlinear phase shift acquired in passing through the sample is much smaller than unity.

Here are some suggestions on how to proceed. Begin with the expression for a gaussian laser beam. Determine first how the beam will be modified in passing thought the nonlinear material. Note that under the assumed conditions the beam diameter at the sample will be unchanged, but that the wavefront curvature will be modified by nonlinear refraction. Note that the modified beam itself approximates a gaussian beam, but with a different value of the wavefront radius of curvature. By assuming that this beam propagates according to the same laws that govern the propagation of a gaussian beam, determine its on-axis intensity in the far field as a function of $z - z_0$.

Note that a more detailed analysis of the z-scan procedure (Sheik-Bahae et al., *IEEE J. Quantum Electron.* 26, 760, (1990)) leads to the somewhat different result

$$\frac{\Delta I}{I} = \frac{4\Phi_{\max} x}{(x^2+1)(x^2+9)}, \quad x = 2(z - z_0)/b, \tag{7.5.34}$$

where $\Phi_{\max}$ is the nonlinear phase shift on-axis when the sample is at the beam waist of the incident laser beam. Plot the functional dependence of both your result and the literature result.

4. *Optical phase conjugation.* Solve the following coupled equations for the boundary conditions that $A_3(0)$ and $A_4(L)$ are arbitrary:

$$\frac{dA_3}{dz} = -\alpha_3 A_3 - i\kappa_4^* A_4^*,$$
$$\frac{dA_4}{dz} = \alpha_4 A_4 + i\kappa_3^* A_3^*.$$

(These equations generalize Eqs. (7.2.31) and describe four-wave mixing in the usual phase conjugation geometry for the case of a lossy medium.)

5. *Optical phase conjugation.* Same as Problem 4, but with the inclusion of phase-mismatch factors so that the coupled equations are given by

$$\frac{dA_3}{dz} = -\alpha_3 A_3 - i\kappa_4^* A_4^* e^{i\Delta k z},$$
$$\frac{dA_4}{dz} = \alpha_4 A_4 + i\kappa_3^* A_3^* e^{-i\Delta k z}$$

where $\Delta k = (\mathbf{k_1} + \mathbf{k_2} - \mathbf{k_3} - \mathbf{k_4}) \cdot \hat{\mathbf{z}}$, and $\mathbf{k_1}$ and $\mathbf{k_2}$ are the wavevectors of the two pump waves.

6. *Optical phase conjugation.* Derive an expression for the phase-conjugate reflectivity obtained by degenerate four-wave mixing utilizing the nonlinear response of a collection of "two-level" atoms. You may make the rotating wave and slowly-varying amplitude approximations and may assume that the amplitudes of the strong pump waves are not modified by the nonlinear interaction.
   [Hint: This problem can be solved using the formalism developed in Section 6.3. This problem has been solved in the scientific literature, and the solution is given by R.L. Abrams and R.C. Lind, *Opt. Lett.* 2, 94 (1978) and 3, 205 (1978).]
7. *Polarization properties of phase conjugation.* Verify Eq. (7.2.41).
8. *Optical bistability.* The discussion of absorptive optical bistability presented in the text assumed that the incident laser frequency was tuned to a cavity resonance. Generalize this treatment by allowing the cavity to be mistuned from resonance, so that the factor $\rho^2 e^{2ikl}$ appearing in the denominator of Eq. (7.3.3) can be set equal to $Re^{i\delta_0}$, where δ_0 is the cavity mistuning in radians.
   [Ans.: Eq. (7.3.10) must be replaced by

$$TI_1 = I_2\left[1 - 2R\left(1 - \frac{C_0 T/R}{1 + 2I_2/I_s}\right)\cos\delta_0 + R^2\left(1 - \frac{C_0 T/R}{1 + 2I_2/I_s}\right)^2\right].$$

   Examination of this expression shows that larger values of C_0 and I_2 are required in order to obtain optical bistability for $\delta_0 \neq 0$.]
9. *Optical bistability.* The treatment of absorptive bistability given in the text assumed that the absorption decreased with increasing laser intensity according to

$$\alpha = \frac{\alpha_0}{1 + I/I_s}.$$

   In fact, many saturable absorbers are imperfect in that they do not saturate all the way to zero; the absorption can better be represented by

$$\alpha = \frac{\alpha_0}{1 + I/I_s} + \alpha_1,$$

   where α_1 is constant. How large can α_1 be (for given α_0) and still allow the occurrence of bistability? Use the same approximations used in the text, namely that $\alpha \ll 1$ and that the cavity is tuned to exact resonance. How are the requirements on the intensity of the incident laser beam modified by a nonzero value of α_1?
10. *Optical bistability.* By means of a graphical analysis of the sort illustrated in Fig. 7.3.5, make a plot of the transmitted intensity I_3 as a function of the incident intensity I_1. Note that more than two stable solutions can occur for a device that displays refractive bistability.

11. *Optical bistability.* Consider refractive bistability in a nonlinear Fabry–Perot interferometer. Assume that the nonlinear material also displays (linear) absorption. How are the intensity requirements for switching modified by the inclusion of loss, and how large can the absorption be and still allow the existence of bistability?
12. *Optical switching.* Show that any physically realizable beam splitter must obey the relation (7.3.21).
13. *Two-beam coupling.* According to Section 7.4, the equations governing the growth of two beams subject to two-beam coupling can be written

$$\frac{dI_1}{dz} = \beta I_1 I_2,$$
$$\frac{dI_2}{dz} = -\beta I_1 I_2.$$

Solve this system for $I_2(z)$ in terms of $I_2(0)$ and the total intensity $I = I_1 + I_2$. (This is not difficult, but you may need to refer to a textbook on differential equations.) Make a sketch of $I_2(z)$ for the cases $\beta > 0$ and $\beta < 0$. What is β, both mathematically and physically?

14. *Self-phase modulation.* The analysis of self-phase modulation that led to Fig. 7.5.1 assumed that the medium had instantaneous response and that the temporal evolution of the pulse had a symmetric waveform. In this case the spectrum of the pulse is seen to broaden symmetrically. How is the spectrum modified for a medium with a sluggish response (given, for example, by Eq. (7.4.7) with τ much longer than the pulse duration)? How is the spectrum modified if the pulse waveform is not symmetric (a sawtooth waveform, for example)?
15. *Pulse propagation.* How is the pulse propagation equation (7.5.32) modified if the quantity $k^2 - k_0^2$ is not approximated by $2k_0(k - k_0)$, as was done in going from Eq. (7.5.18) to Eq. (7.1.19)?
[Ans.: k_2 in Eq. (7.5.32) must be replaced by $(k_1^2 + 2k_0k_2)/2k_0$.]
Why is it that this new equation seems to predict that pulses will spread as they propagate, even when both k_2 and γ vanish?
16. *Temporal solitons.* Verify that the solution given by Eqs. (7.5.33) does in fact satisfy the pulse propagation equation (7.5.32).
17. *Temporal solitons.* Calculate the peak power and energy of an optical soliton with $\tau_0 =$ 10 psec propagating in a silica-core optical fiber of 8 μm core diameter at a wavelength of 1.55 μm.
[Solution: Using the typical values $k_2 = -20$ psec^2/km and $n_2 = 3 \times 10^{-16}$ cm^2/W, we find that $P = 80$ mW and $Q = 0.8$ pJ. Note also that the full width of the pulse measured at half intensity points is equal to $1.76\tau_0$.]

18. *Self-induced transparency*. Optical solitons can also be formed as a consequence of the resonant nonlinear optical response of a collection of two-level atoms. Show that, in the absence of damping effects and for the case of exact resonance, the equations describing the propagation of an optical pulse through such a medium are of the form

$$\frac{\partial \tilde{A}}{\partial z} + \frac{1}{c}\frac{\partial \tilde{A}}{\partial t} = \frac{2\pi i \omega N}{c} p,$$
$$\frac{dp}{dt} = -\frac{i}{\hbar}|\mu|^2 \tilde{A} w, \qquad \frac{dw}{dt} = \frac{-4i}{\hbar}\tilde{A} p$$

(where the atomic response is described as in Section 6.4). Show that these equations yield soliton-like solutions of the form

$$\tilde{A}(z,t) = \frac{\hbar}{\mu \tau_0} \operatorname{sech}\left(\frac{t - z/v}{\tau_0}\right),$$
$$w(z,t) = -1 + 2\operatorname{sech}^2\left(\frac{t - z/v}{\tau_0}\right),$$
$$p(z,t) = -i\mu \operatorname{sech}\left(\frac{t - z/v}{\tau_0}\right)\tanh\left(\frac{t - z/v}{\tau_0}\right)$$

as long as the pulse width and pulse velocity are related by

$$\frac{c}{v} = 1 + \frac{2\pi N \mu^2 \omega \tau_0^2}{\hbar}.$$

What is the value (and the significance) of the quantity

$$\int_{-\infty}^{\infty} \frac{2\mu}{\hbar}\tilde{A}(z,t)dt?$$

(For the case of an inhomogeneously broadened medium, the equations are still satisfied by a sech pulse, but the relation between v and τ_0 is different. See, for example, Allen and Eberly, 1975.)

19. *Modulational instability.* The intent of this problem is to determine the conditions under which the propagation of a monochromatic laser field inside an optical fiber is unstable to the growth of new frequency components. Base your analysis on the nonlinear Schrödinger equation (NLSE) in the form of Eq. (7.5.32). First note that the solution to the NLSE for an input in the form of a cw monochromatic wave is the input field multiplied by an exponential phase factor describing a nonlinear phase shift.

One next wants to determine if this solution is stable to growth of weak perturbations. Assume that the total field within the fiber has the form of the strong component of amplitude A_0 and frequency ω and two weak sidebands symmetrically displaced by frequency δ such that the total field within the fiber can be represented as

$$A(z,\tau) = A_0(z) + A_1(z)e^{-i\delta\tau} + A_2(z)e^{i\delta\tau}.$$

(Here we have dropped the tilde and the subscript s for notational convenience.) Derive the differential equations satisfied by each of the field amplitudes by linearizing the equations in A_1 and A_2. Note that A_1 and A_2 are coupled by four-wave mixing interactions. Determine the conditions for instability to occur by determining when the simultaneous solution to the equations for the A_1 and A_2 fields will experience exponential growth. For what relative sign of n_2 and k_2 can this instability exist? Sketch the dependence of the gain on the sideband detuning δ for various values of the pump amplitude A_0. Also determine the "eigenvector" associated with the exponentially growing solution, that is, the particular linear combination of A_1 and A_2 that experiences exponential growth. Describe the nature of the modulation present on the transmitted field for this particular eigenvector.

Thought question: Why does your solution depend on the group velocity, not the phase velocity, considering that we have analyzed this situation under continuous-wave conditions?

References

Section 7.1 Self-Focusing of Light and Other Self-Action Effect

Aitchison, J.S., et al., 1991. J. Opt. Soc. Am. B 8, 1290.

Barthelemy, A., Maneuf, S., Froehly, C., 1985. Opt. Commun. 55, 201.

Bennink, R.S., Wong, V., Marino, A.M., Aronstein, D.L., Boyd, R.W., Stroud Jr., C.R., Lukishova, S., Gauthier, D.J., 2002. Phys. Rev. Lett. 88, 113901.

Bespalov, V.I., Talanov, V.I., 1966. JETP Lett. 3, 471.

Bjorkholm, J.E., Ashkin, A., 1974. Phys. Rev. Lett. 32, 129.

Boyd, R.W., Lukishova, S.G., Shen, Y.R. (Eds.), 2009. Self-Focusing, Past and Present. Springer, Berlin.

Chiao, R.Y., Garmire, E., Townes, C.H., 1964. Phys. Rev. Lett. 13, 479.

Chiao, R.Y., Kelley, P.L., Garmire, E., 1966. Phys. Rev. Lett. 17, 1158.

Fibich, G., Gaeta, A.L., 2000. Opt. Lett. 25, 335.

Haus, H.A., 1966. Appl. Phys. Lett. 8, 128.

Hercher, M., 1964. J. Opt. Soc. Am. 54, 563.

Kelley, P.L., 1965. Phys. Rev. Lett. 15, 1005.

Loy, M.M.T., Shen, Y.R., 1973. IEEE J. Quantum Electron. 9, 409.

Shen, Y.R., 1975. Prog. Quantum Electron. 4, 1.

Yariv, A., 1975. Quantum Electronics. Wiley, New York, p. 498.

Suggested Additional Reading on Self-Action Effects

Akhmanov, S.A., Khokhlov, R.V., Sukhorukov, A.P., 1972. In: Arecchi, F.T., Schulz-Dubois, E.O. (Eds.), Laser Handbook. North-Holland.

Marburger, J.H., 1975. Prog. Quantum Electron. 4, 35.

Svelto, O., 1974. In: Wolf, E. (Ed.), Progress in Optics XII. North-Holland.

Section 7.2 Optical Phase Conjugation

Bloom, D.M., Bjorklund, G.C., 1977. Appl. Phys. Lett. 31, 592.
Boyd, R.W., Grynberg, G., 1992. Optical phase conjugation. In: Agrawal, G.P., Boyd, R.W. (Eds.), Contemporary Nonlinear Optics. Academic Press, Boston.
Fisher, R.A. (Ed.), 1983. Optical Phase Conjugation. Academic Press, New York.
Gaeta, A.L., Boyd, R.W., 1988. Phys. Rev. Lett. 60, 2618.
Hellwarth, R.W., 1977. J. Opt. Soc. Am. 67, 1.
MacDonald, K.R., Tompkin, W.R., Boyd, R.W., 1988. Opt. Lett. 13, 663.
Maki, J.J., Davis, W.V., Boyd, R.W., Sipe, J.E., 1992. Phys. Rev. A 46, 7155.
Yariv, A., Pepper, D.M., 1977. Opt. Lett. 1, 16.
Zel'dovich, B.Ya., Pilipetsky, N.F., Shkunov, V.V., 1985. Principles of Phase Conjugation. Springer-Verlag, Berlin.

Polarization Properties of Phase Conjugation

Grynberg, G., 1984. Opt. Commun. 48, 432.
Kauranen, M., Gauthier, D.J., Malcuit, M.S., Boyd, R.W., 1989. Phys. Rev. A 40, 1908.
Malcuit, M.S., Gauthier, D.J., Boyd, R.W., 1988. Opt. Lett. 13, 663.
Martin, G., Lam, L.K., Hellwarth, R.W., 1980. Opt. Lett. 5, 186.
Zel'dovich, B.Ya., Shkunov, V.V., 1979. Sov. J. Quantum Electron. 9, 379.

Section 7.3 Optical Bistability

Gibbs, H.M., 1985. Optical Bistability. Academic Press, New York.
Gibbs, H.M., McCall, S.L., Venkatesan, T.N., 1976. Phys. Rev. Lett. 36, 1135.
Lugiato, L.A., 1984. Theory of optical bistability. In: Wolf, E. (Ed.), Progress in Optics XXI. North-Holland.
Stegeman, G.I., Miller, A., 1993. Physics of all-optical switching devices. In: Midwinter, J.E. (Ed.), Photonic Switching, vol. 1. Academic Press, Boston.
Szöke, A., Daneu, V., Goldhar, J., Kurnit, N.A., 1969. Appl. Phys. Lett. 15, 376.

Section 7.4 Two-Beam Coupling

Feinberg, J., 1983. In: Fisher, R.A. (Ed.), Optical Phase Conjugation. Academic Press, New York.
Silberberg, Y., Bar-Joseph, I., 1982. Phys. Rev. Lett. 48, 1541.
Silberberg, Y., Bar-Joseph, I., 1984. J. Opt. Soc. Am. B 1, 662.

Section 7.5 Pulse Propagation and Temporal Solitons

Agrawal, G.P., 1989. Nonlinear Fiber Optics. Academic Press, Boston.
Allen, L.D., Eberly, J.H., 1975. Optical Resonance and Two-Level Atoms. Wiley, New York.
Brewer, R.G., 1967. Phys. Rev. Lett. 19, 8.
Cheung, A.C., Rank, D.M., Chiao, R.Y., Townes, C.H., 1968. Phys. Rev. Lett. 20, 786.
Kim, K.S., Stolen, R.H., Reed, W.A., Quoi, K.W., 1994. Opt. Lett. 19, 257.
Mollenauer, L.F., Stolen, R.H., Gordon, J.P., 1980. Phys. Rev. Lett. 45, 1095.
Shen, Y.R., Yang, G., 2006. In: Alfano, R.R. (Ed.), The Supercontinuum Laser Source. Springer, NY, Chapter 2.
Shimizu, F., 1967. Phys. Rev. Lett. 19, 1097.
Zakharov, V.E., Shabat, A.B., 1972. Sov. Phys. JETP 34, 63.